

The Chemical Synthesis of Discodermolide

I. Paterson and G.J. Florence

Abstract The marine sponge-derived polyketide discodermolide is a potent antimitotic agent that represents a promising natural product lead structure in the treatment of cancer. Discodermolide shares the same microtubule-stabilising mechanism of action as Taxol®, inhibits the growth of solid tumours in animal models and shows synergy with Taxol. The pronounced cytotoxicity of discodermolide, which is maintained against cancer cell lines that display resistance to Taxol and other drugs, combined with its scarce availability from its natural source, has fuelled significant academic and industrial interest in devising a practical total synthesis as a means of ensuring a sustainable supply for drug development. This chapter surveys the various total syntheses of discodermolide that have been completed over the period 1993–2007, focusing on the strategies employed for introduction of the multiple stereocentres and achieving control over the alkene geometry, along with the various methods used for realising the pivotal fragment couplings to assemble progressively the full carbon skeleton. This dedicated synthetic effort has triumphed in removing the supply problem for discodermolide, providing sufficient material for extensive biological studies and enabling its early stage clinical development, as well as facilitating SAR studies for lead optimisation.

Keywords Anticancer, Natural products, Polyketides, Stereocontrol, Tubulin

Contents

1	Introduction.....	74
1.1	Isolation and Structure of Discodermolide.....	74
1.2	Biology of Discodermolide	75

I. Paterson (✉)

University Chemical Laboratory, Lensfield Road, Cambridge, CB2 1EW UK
e-mail: ip100@cam.ac.uk

G.J. Florence

School of Chemistry and Centre for Biomolecular Sciences, University of St Andrews,
North Haugh, St Andrews, KY16 9ST UK

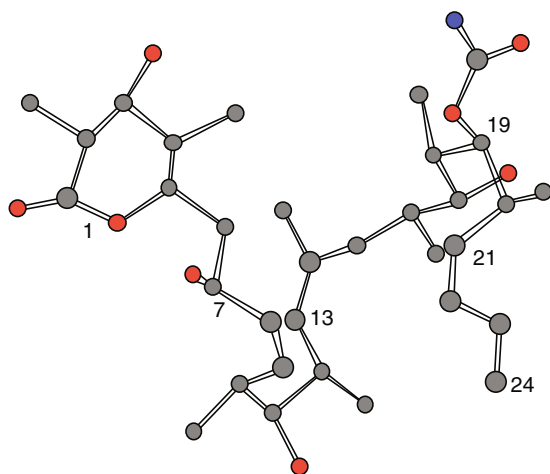
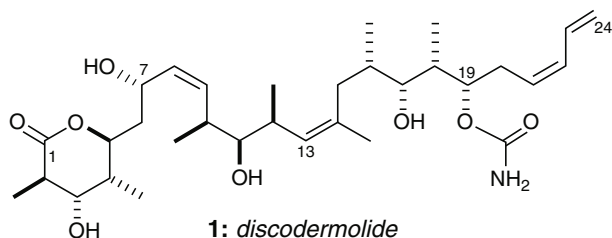
2	Total Synthesis	77
2.1	Schreiber Total Synthesis	77
2.2	Smith Total Syntheses	79
2.3	Myles Total Synthesis	89
2.4	Marshall Total Synthesis	91
2.5	Paterson Total Synthesis	96
2.6	Panek Total Synthesis	104
2.7	Ardisson Total Synthesis	106
2.8	Novartis Process Chemistry Group Synthesis	108
3	Summary	114
	References	114

1 Introduction

The marine ecosystem provides an extensive source of structurally diverse natural products isolated from numerous organisms including algae, molluscs, corals, sponges, tunicates and phytoplankton, as well as associated microorganisms [1–4]. The biological activity of these compounds is often startling, demonstrating, for example, potent cytotoxic, immunosuppressive and antibiotic properties making them of interest to the pharmaceutical industry [5–8]. However, the low natural abundance of many of these lead structures means that realistic and practical synthetic routes are required to provide material to investigate and exploit further their biological activity [8, 9]. These factors, combined with the exquisite molecular architectures that many of these compounds possess, offer demanding challenges to the modern synthetic chemist. In particular, the marine polyketide discodermolide (**1**, Fig.1) has inspired intense synthetic activity, due to its biological profile and potential as a new generation anticancer agent given the onset of multidrug resistance in established cancer chemotherapies (see [10–13] for previous reviews on the synthesis of discodermolide; see [14] for a recent review on the synthesis of bioactive marine polyketides; see [15, 16] for an excellent recent review of microtubule-stabilising natural products).

1.1 Isolation and Structure of Discodermolide

Discodermolide (**1**) is a unique polyketide isolated by Gunasekera and co-workers at the Harbor Branch Oceanographic Institution in 1990 from the Caribbean deep-sea sponge *Discodermia Dissoluta* [17, 18]. This sponge was collected at a depth of 33m and several other new *Discodermia* species containing discodermolide were collected by manned submersibles at depths between 185 and 220m. These samples were exhaustively extracted and purified to provide discodermolide in an initial isolation yield of 0.002wt% from frozen sponge. Its gross structure was determined by extensive spectroscopic studies and the relative configuration was established by single crystal X-ray crystallography as shown in Fig.1. Structurally, discodermolide bears 13 stereogenic centres, a tetrasubstituted δ -lactone (C1–C5), one di- and one



X-ray structure of discodermolide (**1**).
Hydrogens omitted for clarity

Fig.1 Structure of discodermolide

tri-substituted (*Z*)-double bond, a carbamate moiety (C19) and a terminal (*Z*)-diene (C21–C24). Discodermolide adopts a U-shaped conformation in the solid state, where the (*Z*)-olefins at C13–C14 and C8–C9 act as conformational locks by minimising A(1,3) strain between their respective substituents. The δ -lactone adopts a boat-like conformation with H-bonding between the lactone moiety and the C7-OH group, which is retained in solution [19].

1.2 Biology of Discodermolide

Discodermolide was initially reported to be a potent immunosuppressive agent, both in vivo and in vitro, comparable with FK-506 and rapamycin, as well as displaying antifungal activity. It inhibited T-cell proliferation with an IC_{50} of 9nM in the mixed leukocyte reaction and graft vs host disease in transplanted mice [20, 21]. Further biological screening revealed pronounced cytotoxicity, causing cell cycle arrest at the G2/M phase in a variety of human and murine cell lines, with

IC_{50} values ranging from 3 to 80nM. In a similar fashion to Taxol, discodermolide functions by microtubule stabilisation, halting mitosis and causing cell death by apoptosis [22]. Discodermolide is an important member of a unique group of secondary metabolites (Fig.2) that act as microtubule-stabilising agents and mitotic spindle poisons, which currently include Taxol (paclitaxel) (**2**) [23], epothilones A (**3**) and B (**4**) [24], sarcodictyin A (**5**) [25], eleutherobin (**6**) [26], laulimalide (**7**) [27], FR182877 (cyclostreptin) (**8**) [28], peloruside A (**9**) [29], dictyostatin (**10**) [30–32] and the semi-synthetic Taxol analogue, Taxotere (**11**) [33]. Despite the lack of structural similarities, the cytotoxicity and microtubule stabilising properties of discodermolide are comparable to Taxol. Moreover, the growth of Taxol-resistant ovarian and colon carcinoma cells are inhibited by discodermolide ($IC_{50} < 2.5nM$) [34]. Initial investigations into determining the discodermolide binding site through competition studies with radiolabelled Taxol suggested it occupied an identical or similar binding site on β -tubulin [35]. In comparative studies with the Taxol-dependent human lung carcinoma cell line A549-T12, discodermolide was unable to act as a substitute for Taxol, whereas the epothilones and eleutherobin were able to maintain the viability of the cell line [36]. Significantly, a synergistic potentiation of discodermolide's cytotoxicity was observed, when used in combination with Taxol, suggesting that discodermolide may bind to tubulin at a distinct site from Taxol. More recent *in vivo* studies on ovarian tumour xenograft bearing mice have also shown this synergy, inducing tumour regression without toxicity to the mouse [37]. Notably, these studies suggest that the synergistic combination of Taxol and discodermolide may offer a useful therapy, minimising the plethora of

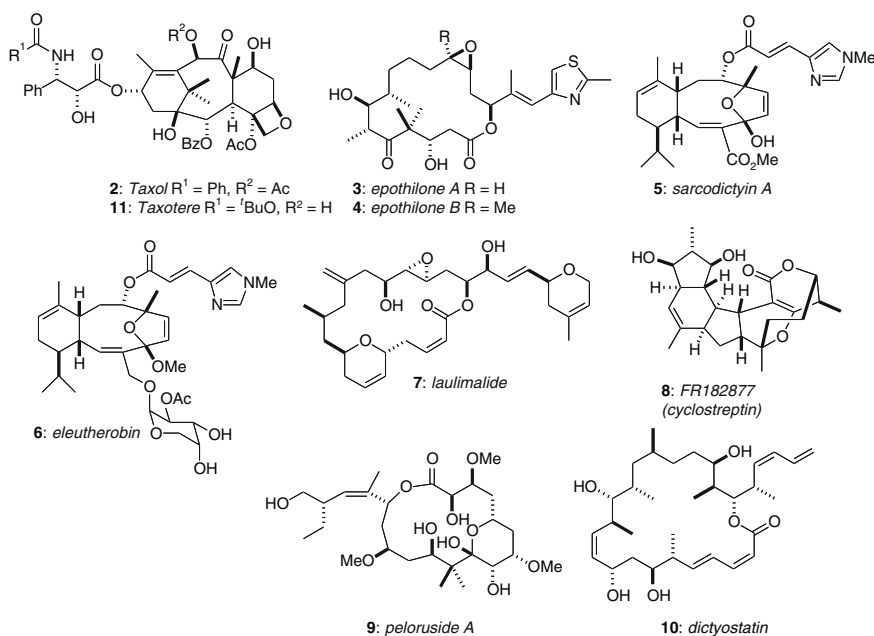


Fig. 2 Structures of other microtubule-stabilizing natural products

toxicity related side-effects that are observed in the clinic with high doses of Taxol. In 2006, the group of Carlomagno elucidated the bioactive conformation of discodermolide bound to soluble tubulin by using elegant NMR studies and proposed a common pharmacophore with the epothilones [38].

The highly encouraging biological profile of discodermolide led it to become a promising candidate for clinical development as a chemotherapeutic agent for breast cancer and other multi-drug-resistant cancers. This potential was recognised by Novartis Pharma AG, who licensed discodermolide from the Harbor Branch Oceanographic Institution and launched an impressive large-scale total synthesis campaign to supply material for clinical trials for the treatment of advanced solid malignancies. However, these trials have since been halted due to toxicity associated with the chemotherapy [39].

2 Total Synthesis

While the early clinical development of Taxol was severely hampered by the supply problem, this was eventually resolved by semi-synthesis from 10-deacetyl baccatin III, obtained from the needles of the common European yew tree. In comparison, the epothilones, which are currently in advanced clinical trials as anticancer agents, are obtained by fermentation [40]. Ixemptra®, the lactam analogue of epothilone B which is obtained by semi-synthesis, has recently been approved by the FDA in the United States for the treatment of advanced breast cancer [41]. Unfortunately, a fermentation process is not as yet possible for discodermolide, even though as a polyketide it is presumably produced by a symbiotic microorganism associated with the sponge source (see [42] for a review on symbiotic bacteria as a source of marine natural products). Therefore, the supply problem for discodermolide could only be resolved via total synthesis. Consequently, there has been considerable synthetic effort directed towards discodermolide, culminating in 13 completed total syntheses reported by 8 groups [43–55] and numerous fragment syntheses [55–97]. This chapter highlights the total syntheses of discodermolide by ourselves and the groups of Schreiber, Smith, Myles, Marshall, Panek, Ardisson, and the Novartis process chemistry team in Basel led by Mickel. The key carbon-carbon bond disconnection strategies employed in all these approaches are highlighted in Fig.3. In particular, we focus on the strategies employed to configure the multiple stereogenic centres, the methods employed to introduce the synthetically challenging (*Z*)-olefins and the pivotal fragment coupling steps.

2.1 Schreiber Total Synthesis

Schreiber and co-workers reported the first total synthesis of (–)-discodermolide (*ent*-1) in 1993, confirming the relative stereochemistry and establishing the absolute configuration [43, 44]. In 1996, they reported the first synthesis of the natural

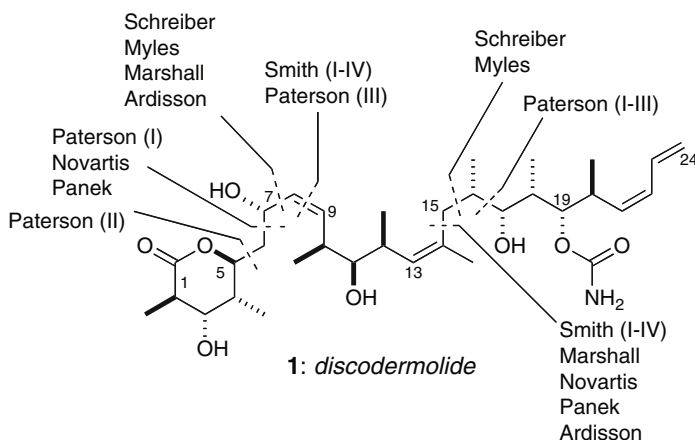
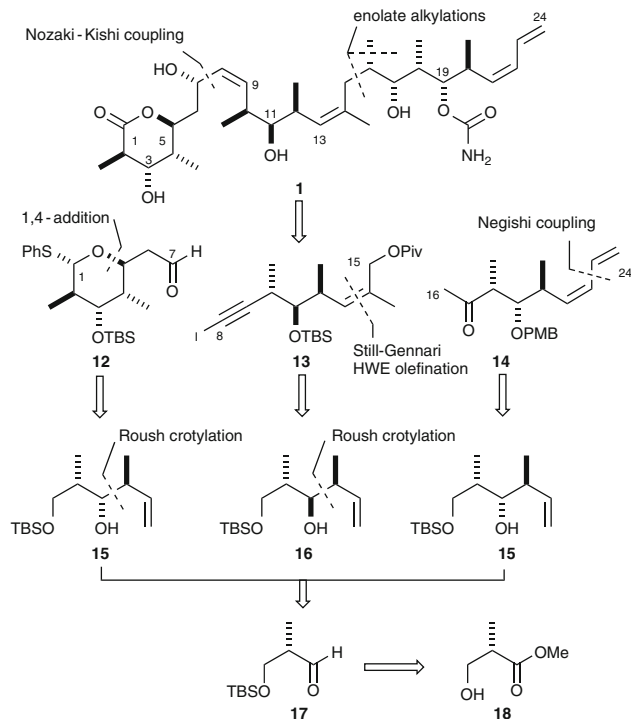


Fig. 3 Key disconnections employed in completed syntheses of discodermolide

antipode (+)-discodermolide (**1**), following an almost identical route performed in the correct enantiomeric series (Scheme 1), along with several analogues designed to study the mode of tubulin binding and microtubule stabilizing properties [44]. Their synthetic strategy towards (+)-discodermolide involved key fragment couplings via Nozaki-Kishi addition [98–101] at C7–C8 and enolate alkylation at C15–C16, requiring the three key subunits **12** (C1–C7), **13** (C8–C15) and **14** (C16–C24). In turn, the homoallylic alcohols **15** and **16** served as building blocks for the subunit synthesis, accessible via Roush crotylation reactions with the aldehyde **17** [102], derived from Roche ester **18** which serves as a starting point in all of the synthetic endeavours reported to date.

The C1–C7 aldehyde **12** was prepared in eight steps starting with the Roush crotylation of aldehyde **17** (Scheme 2) [102]. Ozonolysis and chain extension of **15** provided (*E*)-enoate **19**; the C5 stereocentre was then introduced via an Evans-Prunet hetero-Michael addition [103]. Transformation of **20** into aldehyde **12** was completed in six steps. The C16–C24 methyl ketone **14** was obtained in seven steps from homoallylic alcohol **15**. Protection, ozonolysis and Stork-Wittig olefination [104] of the intermediate aldehyde was followed by a palladium-catalysed Negishi coupling [105] of vinyl iodide **21** with vinyl zinc bromide to introduce the terminal (*Z*)-diene unit in **14**. The synthetically demanding C13–C14 trisubstituted (*Z*)-alkene found in **13** was introduced by Still-Gennari HWE olefination (*Z*:*E*≥20:1) [106], following silyl protection and ozonolysis of **16**. Protecting group manipulations with the resulting (*Z*)-enoate **22** and homologation to iodoacetylene **13** via oxidation, alkylation and iodination at C8 completed the final subunit.

Assembly of the subunits began with the Nozaki-Kishi coupling reaction of iodoacetylene **13** and aldehyde **12**, in the presence of $\text{CrCl}_2/\text{NiCl}_2$, to provide propargylic alcohol **23**, with 3:1 dr at C7 (Scheme 3). The four-step conversion to bromide **24** was followed by the enolate alkylation of methyl ketone **14**.



Scheme 1 Schreiber's synthetic strategy

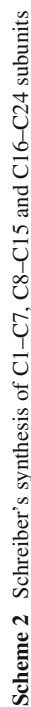
Further alkylation of the lithium (*Z*)-enolate of **25** with methyl iodide gave **26**, introducing the C16 stereocentre (3:1 dr) and completing the carbon backbone. Oxidation at C1 and carbamate formation gave **27** which underwent a chelation-controlled reduction at C17 (30:1 dr). Finally, global deprotection completed the synthesis of discodermolide (**1**), with an overall yield of 4.3% achieved over 24 steps in the longest linear sequence.

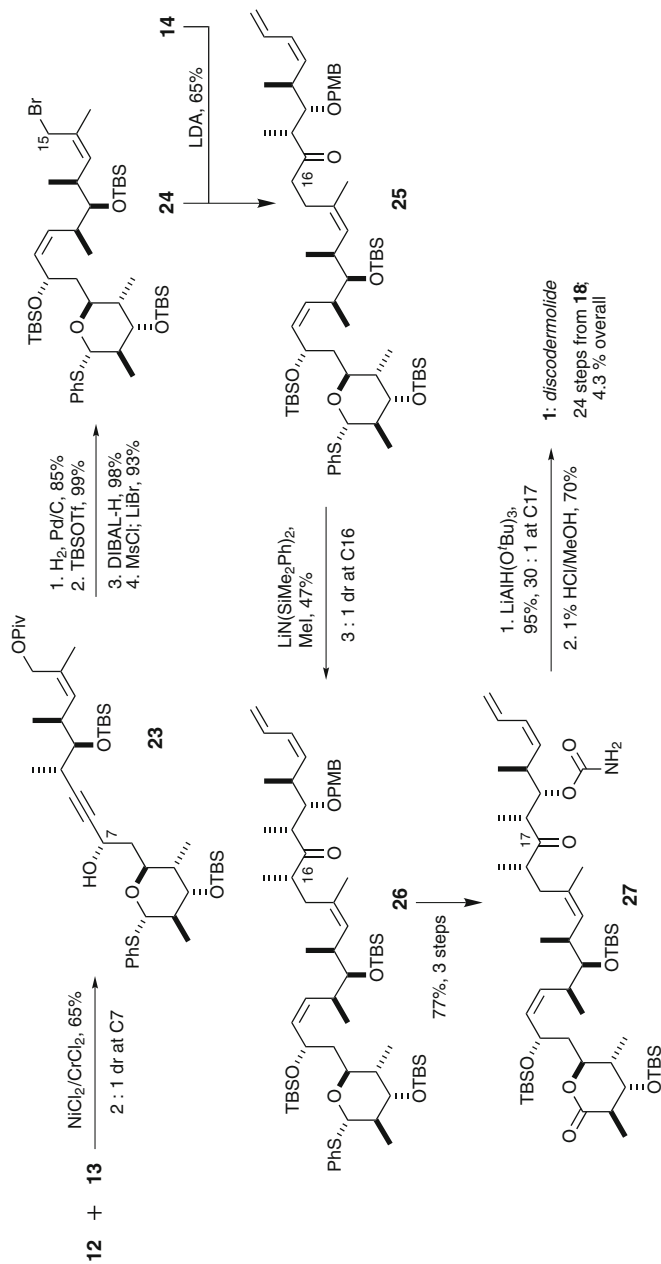
The Schreiber synthesis is particularly noteworthy in that the absolute configuration of discodermolide was assigned unambiguously, and through the preparation of numerous analogues the first structure-activity relationship study was possible [35, 44]. Their synthesis of the unnatural antipode (*ent*-**1**) also led to the unexpected discovery that it causes cell cycle arrest in the S-phase [107].

2.2 Smith Total Syntheses

2.2.1 First Generation (1995)

Smith and co-workers reported their initial synthesis of (–)-discodermolide (*ent*-**1**) in 1995 [45]. They invoked key fragment unions at C8–C9 and C14–C15 via Wittig

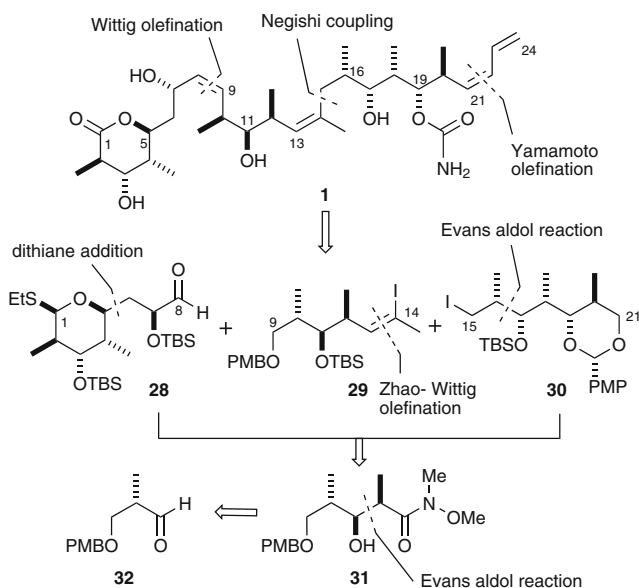


**Scheme 3** Schreiber's subunit assembly and completion of discodermolide

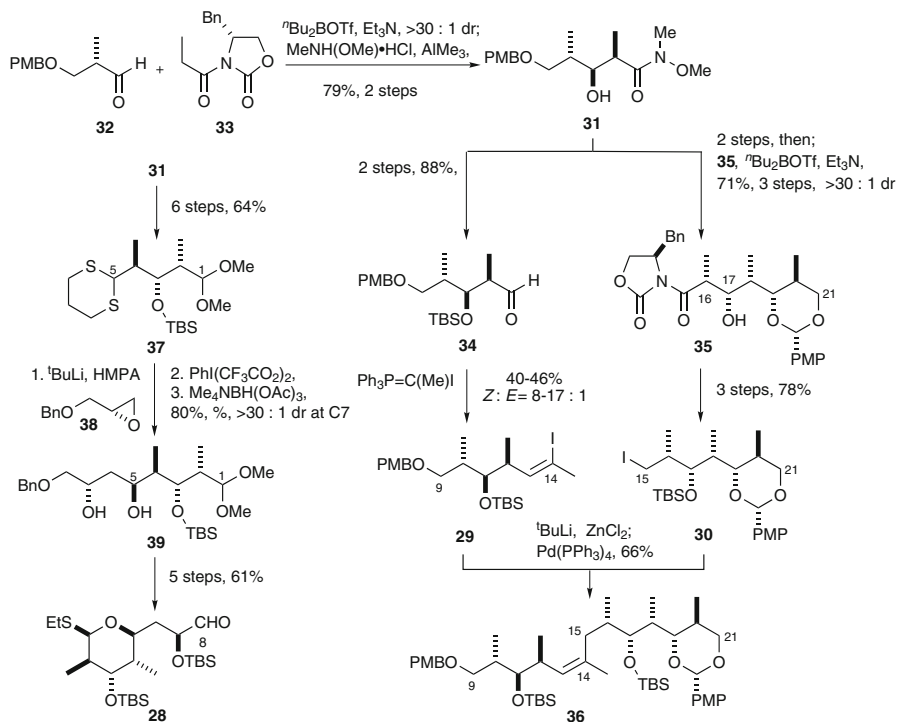
olefination and Negishi cross-coupling [105], respectively (Scheme 4), dividing the carbon skeleton into three key subunits **28** (C1–C8), **29** (C9–C14) and **30** (C15–C21). Smith recognized the repeating stereotriad found in all three subunits and took advantage of a common precursor **31** for fragment synthesis. For clarity of presentation, the Smith first-generation synthesis is shown here in the correct enantiomeric series corresponding to natural (+)-**1**.

The common precursor **31** was configured using the Evans *syn* aldol reaction of propionimide **33** with the aldehyde **32**, available in three steps from Roche ester **18** (Scheme 5) [108–111]. The (*Z*)-alkenyl iodide at C14 was introduced by a Zhao-Wittig olefination on aldehyde **34** in moderate yield with variable selectivity (*Z*:*E* = 8–17:1) [112, 113]. The synthesis of the C15–C21 segment **30** utilized a second Evans aldol reaction to configure the C16–C17 *syn*-relationship to provide **35** which was transformed into iodide **30**. A palladium-catalysed Negishi cross-coupling of the corresponding zincate from the C14 vinyl iodide **29** with iodide **30** then gave the C9–C21 segment **36** [105]. The synthesis of the C1–C8 thioacetal aldehyde **28** began with the six-step elaboration of **31** to dithiane **37**, coupling with epoxide **38** was then followed by dithiane cleavage and Evans-Saksena 1,3-*anti* reduction of the intermediate β -hydroxy ketone to provide **39** [114], and installing the C7 stereocentre. A further 5 steps were then required to access the β -ethylthioacetal aldehyde **28**, giving a total of 14 steps from **31**.

As shown in Scheme 6, the elaboration of the C9–C21 fragment **36** to phosphonium salt **40** proved problematic, requiring the treatment of the intermediate iodide **41** with triphenylphosphine at ultrahigh pressure (12.8kbar) for six days. The (*Z*)-selective Wittig coupling of aldehyde **28** and phosphonium salt **40** then gave the C1–C21 intermediate **42**



Scheme 4 Smith's first-generation strategy



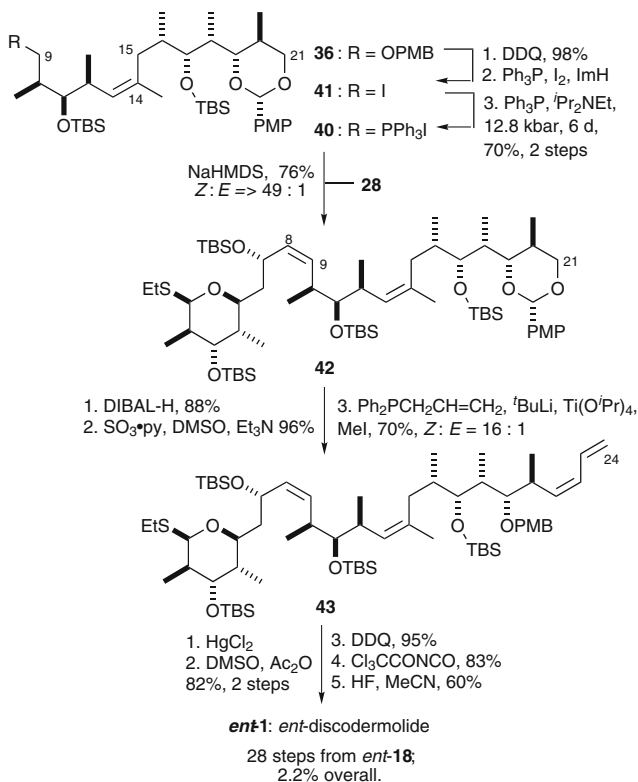
Scheme 5 Smith's synthesis of C1–C8, C9–C14 and C15–21 subunits, and assembly of C8–C21 intermediate

(Z:E = 49:1). At this stage, the (Z)-diene unit was introduced utilizing the Yamamoto olefination protocol to give **43** [115]. A further five steps were then required to complete Smith's first-generation synthesis of (–)-discodermolide (*ent*-**1**), in 2.2% overall yield over 28 steps in the longest linear sequence based on the C1–C8 aldehyde **28**.

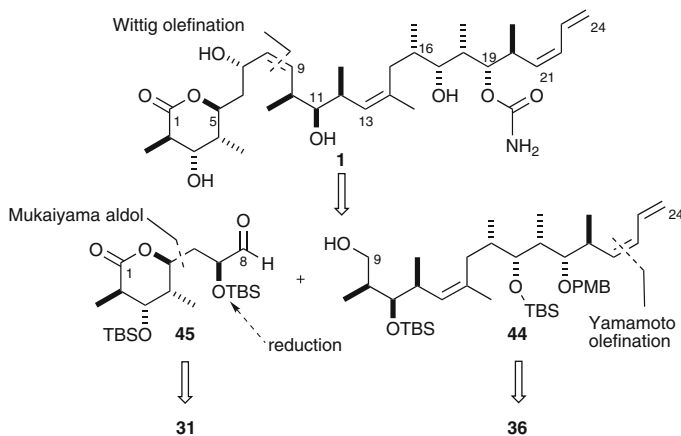
2.2.2 Second Generation (1999)

Smith and co-workers reported their second-generation approach to discodermolide in 1999, which was now performed in the correct enantiomeric series [46–48]. By carefully redesigning the route, the overall number of steps was significantly reduced and, importantly, it enabled a gram-scale synthesis. As outlined in Scheme 7, the key bond constructions at C8–C9 and C14–C15 were retained, while strategic modifications involved the earlier introduction of the terminal (Z)-diene unit in **44** and a revised C1–C8 subunit **45**.

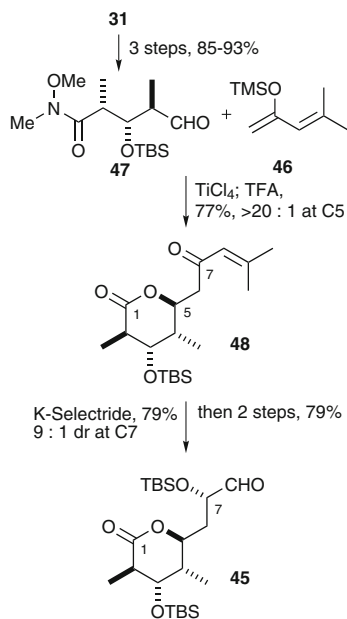
As shown in Scheme 8, the synthesis of aldehyde **45** was achieved in eight steps utilizing the common precursor **31** [46–48]. Remarkably, the Mukaiyama aldol addition of silyl enol ether **46** to aldehyde **47** proceeded with anti-Felkin selectivity, which was attributed to involvement of the Weinreb amide and aldehyde carbonyl



Scheme 6 Smith's first-generation assembly of discodermolide



Scheme 7 Smith's second-generation strategy



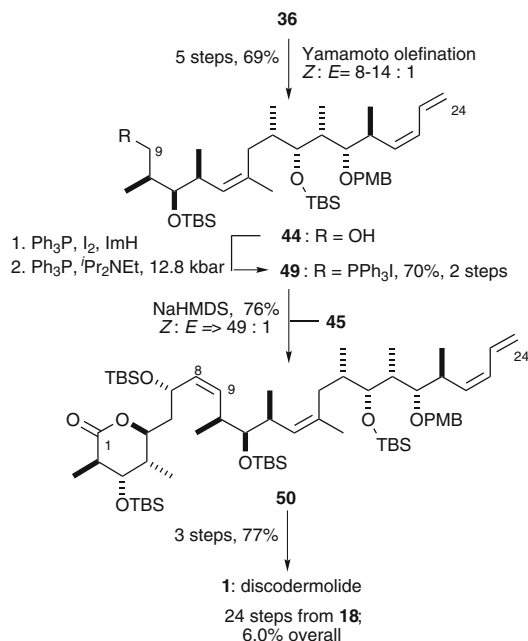
Scheme 8 Smith's synthesis of revised C1–C8 subunit

oxygen in forming an eight-membered chelate with the titanium Lewis acid, and after work-up and acid-catalysed δ -lactonisation with TFA this gave the ketone **48**. K-Selectride reduction at C7 (9:1dr), followed by TBS protection and ozonolysis provided **45**, in 13 steps and 21% overall yield from **18** [70–97].

Starting from the C9–C21 fragment **36**, the installation of the terminal Z-diene unit was achieved in a five-step sequence, in which the Yamatoto olefination gave a Z:E ratio of 8–14:1 (Scheme 9) [115]. The phosphonium salt **49** was prepared from **44** in two steps, again requiring ultrahigh pressure conditions. The Wittig coupling of phosphonium salt **49** and aldehyde **45** then gave **50** (Z:E = 15–24:1). A further three steps were required to complete Smith's second-generation synthesis of discodermolide, which proceeded in an improved 6% yield over 24 steps (longest linear sequence). The Smith second-generation synthesis is notable in that it provided an impressive 1.04 g of discodermolide, enabling extensive biological and preclinical evaluation. However, further scale up of this route would pose significant technical challenges due, in particular, to the limited availability of suitable ultrahigh pressure reactors for performing large-scale preparations of the pivotal phosphonium salt **49**. This limiting factor was then addressed in a third-generation approach [49].

2.2.3 Third Generation (2003)

Although the Smith second-generation synthesis offered several improvements over their initial route, the use of the ultrahigh pressure over extended time periods in the formation of the key Wittig salt **49** severely limited the possibility of further



Scheme 9 Completion of Smith's second-generation synthesis

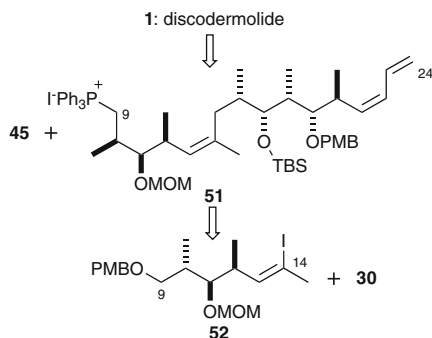
scale-up. Thus, the Smith group's third-generation synthesis addressed this limiting step [49], through the simple replacement of the sterically demanding TBS group at C11 with a MOM group in **51**, while retaining the successful C14–C15 and C8–C9 coupling strategy (Scheme10).

As detailed in Scheme11, a Negishi-type coupling of **30** and the revised C9–C14 subunit **52**, readily derived from **31**, followed by an established sequence gave alcohol **53** [46–48], in preparation for phosphonium salt formation. Conversion into the intermediate iodide and reaction with triphenylphosphine at ambient pressure proceeded smoothly to give **51** in 70% yield. However, Wittig olefination of aldehyde **45** with **51** using methyl lithium/lithium bromide for deprotonation generated the C8–C9 (Z)-olefin with substantially reduced selectivity (third generation = 4:1, *cf* second generation = 24:1). Conversion into discodermolide then required three steps, giving a 1.9% overall yield over 24 steps in the longest linear sequence.

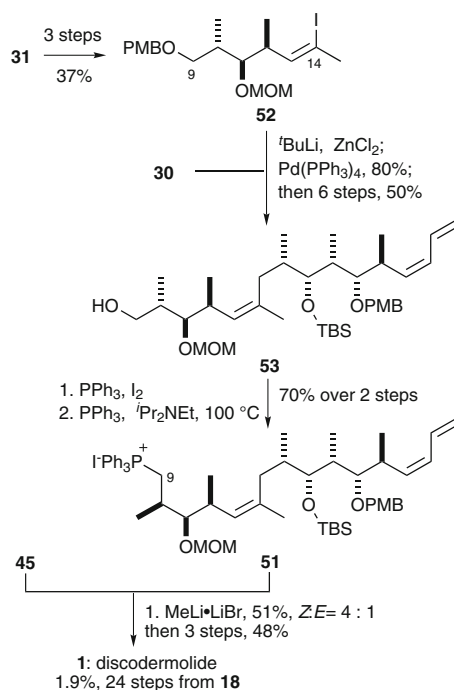
This revised strategy demonstrates that a simple change in hydroxyl protecting groups can markedly influence reactivity and selectivity. While formation of the Wittig salt **51** could now be achieved at atmospheric pressure, its coupling with aldehyde **45** only proceeded in moderate yield and selectivity.

2.2.4 Fourth Generation (2005)

In 2005, Smith and co-workers reported their fourth-generation synthesis of discodermolide [50]. Using the Suzuki-coupling at C13–C14 developed by Marshall [53, 54,

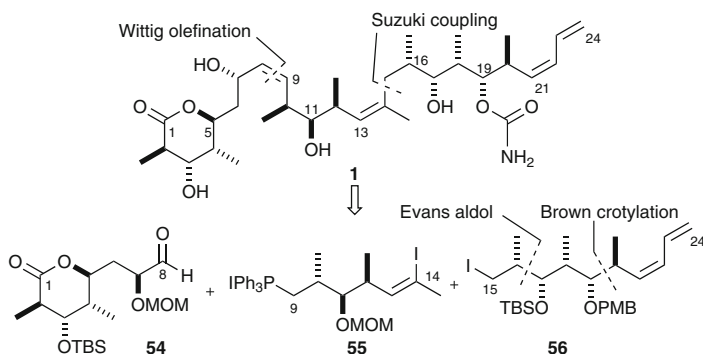


Scheme 10 Smith's third-generation strategy

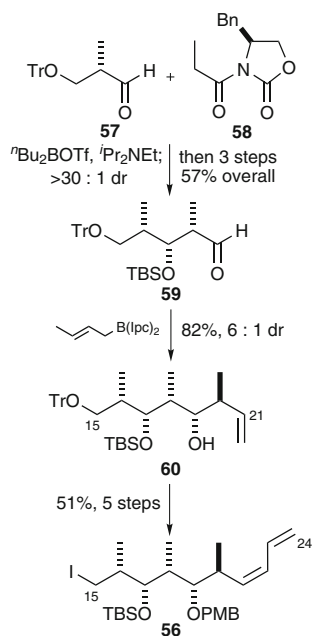


Scheme 11 Smith's third-generation synthesis

116], a revised strategy was devised based on reversing the order of the key fragment couplings. Thus, a Wittig olefination at C8–C9 between a modified C1–C8 aldehyde **54** and phosphonium salt **55** was followed by C14–C15 bond formation with the C15–C24 subunit **56**, as shown in Scheme 12. These modifications were designed to further increase the overall efficiency and convergency of their approach.



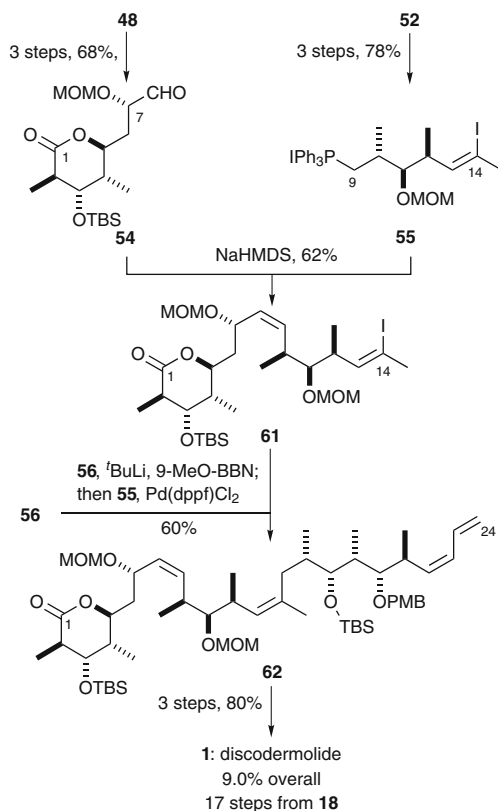
Scheme 12 Smith's fourth-generation strategy



Scheme 13 Smith's synthesis of the C15–C24 subunit

As outlined in Scheme 13, the synthesis of the C15–C24 subunit **56** started with an Evans aldol reaction between the aldehyde **57** and **58** [108–111]. Transformation into aldehyde **59** and a Brown crotylation then gave **60** [117], which was converted into **56** in five steps.

The C1–C8 aldehyde **54** and the C9–C14 Wittig salt **55** were accessed from previously reported intermediates **48** and **52** (Scheme 14). A Wittig olefination of aldehyde **54** with **55** gave the C1–C14 intermediate **61**. In turn, a Suzuki coupling of the boronate derived from **56** with **61** provided **62** [116]. Following their established endgame, the synthesis of discodermolide was now achieved in 9.0% overall yield with 17 steps in the longest linear sequence.

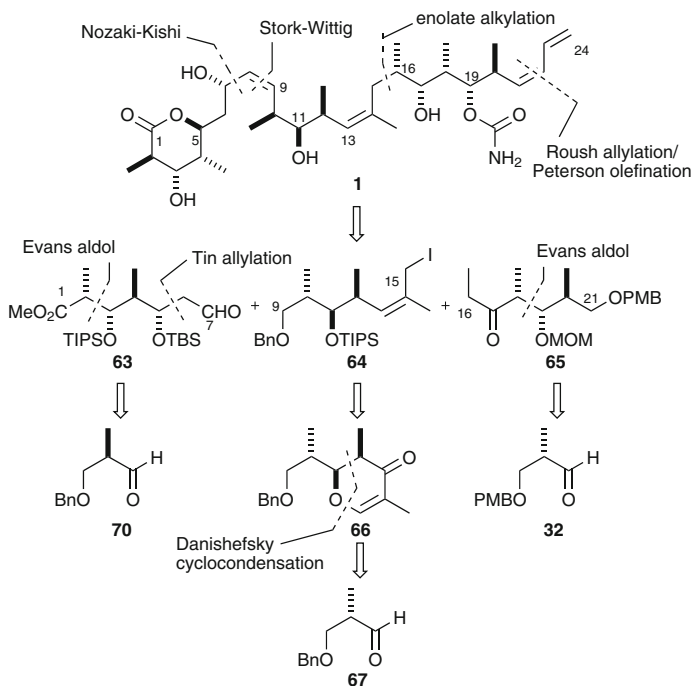


Scheme 14 Completion of Smith's fourth-generation synthesis

2.3 Myles Total Synthesis

Myles and co-workers reported the synthesis of (–)-discodermolide (*ent*-**1**) in 1997 [51]. This was followed by their synthesis of the natural antipode in 2003, exploiting an analogous coupling strategy with improved subunit syntheses, the details of which are presented here [52]. The Myles approach to discodermolide relied on key bond unions at C7–C8 (Nozaki-Kishi) and C15–C16 (enolate alkylation) giving rise to the subunits **63** (C1–C7), **64** (C9–C15), and **65** (C16–C21) (Scheme 15). The synthesis of these subunits utilized a combination of both substrate and reagent controlled reactions, including a novel solution to the installation of the C13–C14 (*Z*)-trisubstituted olefin using the cycloadduct **66** [118].

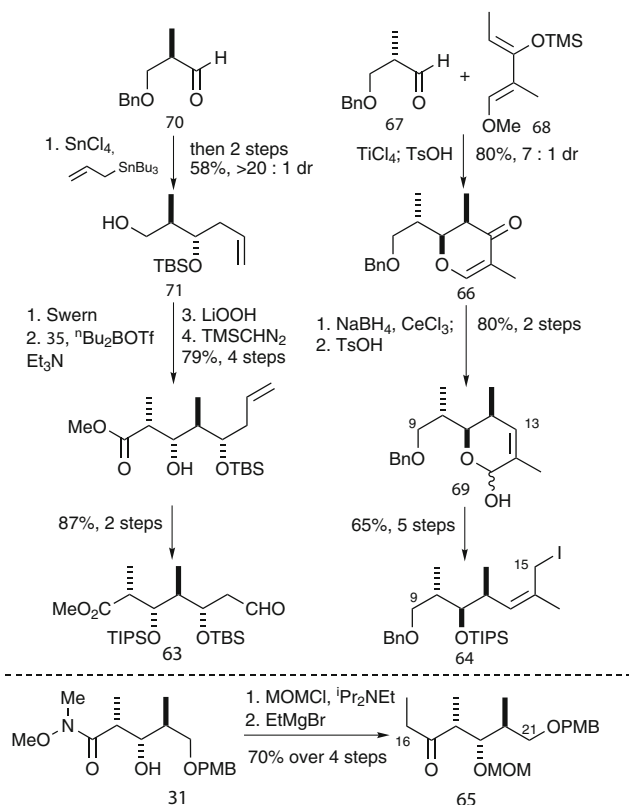
The synthesis of the C9–C15 subunit **64** commenced with the cyclocondensation of aldehyde **67** and diene **68** to provide dihydropyrone **66** (Scheme 16) [118]. A Luche reduction [119, 120] and acid-mediated Ferrier rearrangement gave lactol **69** [121], installing the C13–C14 (*Z*)-trisubstituted olefin. A further five steps



Scheme 15 Myles' synthetic strategy

were then required to access **64**, involving the reductive opening of **69** followed by a series of protecting and functional group manipulations. The C16–C21 subunit **65** was conveniently accessed from the Smith common precursor **33**. Myles' improved synthesis of the C1–C7 subunit **63** began with the tin-mediated allylation [122–124] of **70** under chelation control (>20:1dr), which after silyl protection and debenzoylation provided **71**. The C2 and C3 stereocentres were configured via an Evans aldol reaction [108–111] and the resulting adduct was converted into **63** over four steps.

As shown in Scheme17, Myles' fragment assembly began with the demanding enolate alkylation of ketone **65** with iodide **64** to form the C15–C16 bond, a tactic previously explored by both Schreiber and Heathcock with little success [44, 71]. The combination of MOM protection at C19 in **65** and lithium amide base in a mixed hexanes/THF solvent system proved essential to the success of this alkylation (6:1dr at C16) [51, 52]. A chelation directed reduction of **72** afforded 8:1 selectivity at C17, which after a series of protecting group manipulations provided **73**. A Stork-Wittig olefination (*Z:E* = 20:1) [104] and elaboration into aldehyde **74** was followed by the introduction of the terminal (*Z*)-diene unit via addition of allylboronate **75** and Peterson-type elimination of the resulting 1,2-*anti* hydroxy-silane to give **76** (*Z:E* ≥ 20:1) [125, 126]. Following formation of carbamate **77**, the stage was set for

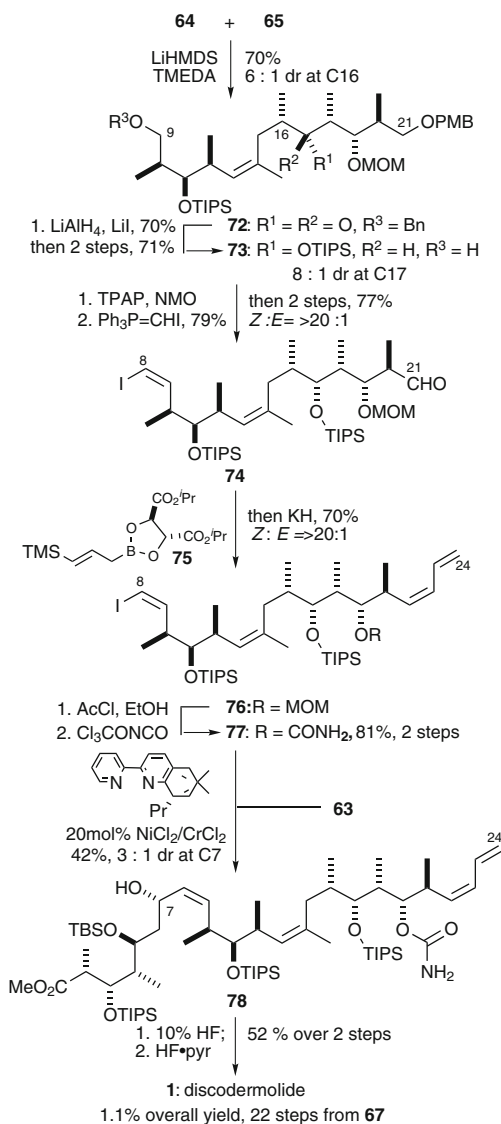


Scheme 16 Myles' synthesis of C1–C7, C9–C15 and C16–C21 subunits

the Nozaki-Kishi coupling with **63**. In Myles' initial synthesis of *ent-1* employing 1mol% $\text{NiCl}_2/\text{CrCl}_2$ in DMSO, this coupling gave low yields and selectivity at C7 (20–40%, 2.5:1dr). However, employing Kishi's chiral bipyridinyl ligand with 20mol% $\text{NiCl}_2/\text{CrCl}_2$ in THF provided adduct **78** in more reliable, albeit moderate, yields with slightly improved selectivity at C7 (3:1dr) [127]. Finally, global deprotection with concomitant δ -lactonization gave discodermolide in 1.1% overall yield over 22 steps in the longest linear sequence from **67**. The Myles synthesis, akin to the Schreiber approach, highlighted the limited utility of the Nozaki-Kishi bond disconnection at C7–C8 in terms of both yield and control over the C7 stereocentre.

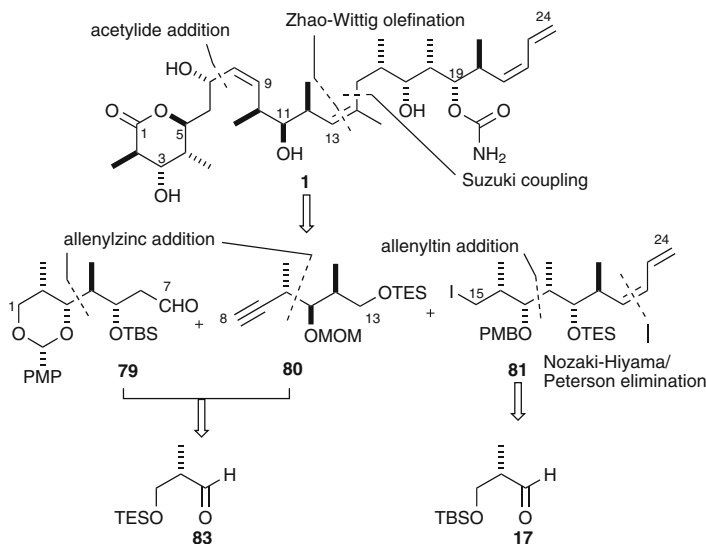
2.4 Marshall Total Synthesis

In 1998, Marshall and co-workers demonstrated the utility of allenyl metal addition methodology for the synthesis of the polypropionate subunits contained in discodermolide [53, 54]. As outlined in Scheme 18, Marshall divided the carbon backbone



Scheme 17 Myles' subunit assembly and completion of discodermolide

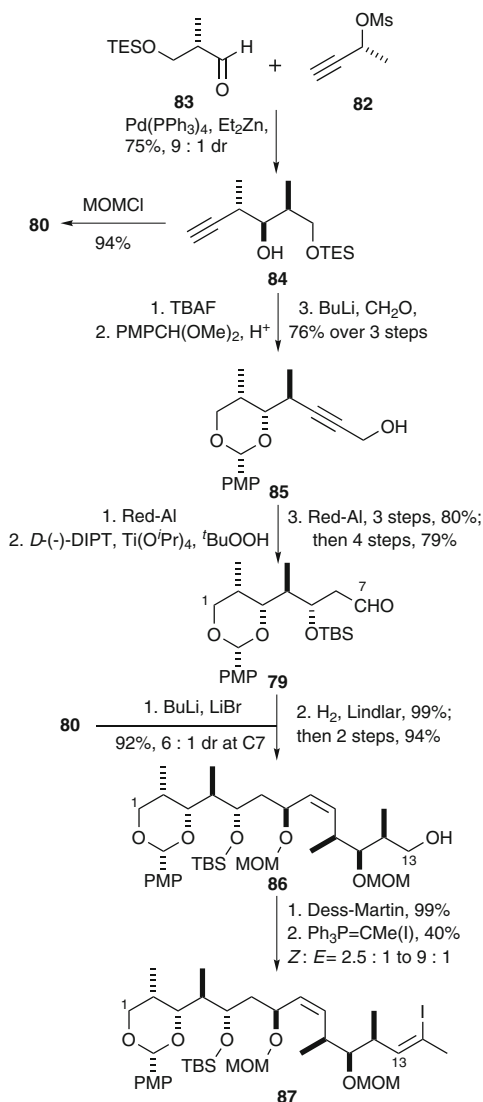
of **1** into three segments **79** (C1–C7), **80** (C8–C13) and **81** (C15–C24), reliant on lithium acetylide addition to an aldehyde at C7–C8 and Suzuki cross-coupling at C14–C15 [116]. This latter bond construction appears to have significant advantages over Smith's Negishi-type coupling due to its greater robustness and scalability, and was subsequently adopted by Novartis in their process development scale-up effort (see Sect. 2.8) [65–69].



Scheme 18 Marshall's synthetic strategy

The synthesis of the C1–C7 and C8–C13 subunits **79** and **80** began with the addition of the chiral allenylzinc species, generated in situ from the treatment of propargylic mesylate **82** with Et_2Zn /catalytic $\text{Pd}(0)$, to aldehyde **83** (Scheme 19) [53, 54]. Completion of the C1–C7 subunit **79** required ten further steps in which **84** was converted into propargylic alcohol **85** and subsequently underwent alkyne reduction, Sharpless epoxidation and directed hydride opening of the resulting epoxide to introduce the C5–OH stereocentrem [54]. Stereoselective addition of the lithium anion of **80–79** (6:1dr at C7), followed by a Lindlar hydrogenation and protecting group adjustments gave **86**. Oxidation and a Zhao–Wittig olefination provided the C1–C14 intermediate **87** in moderate yields with variable *Z:E* ratios ranging from 1.3 to 9:1.

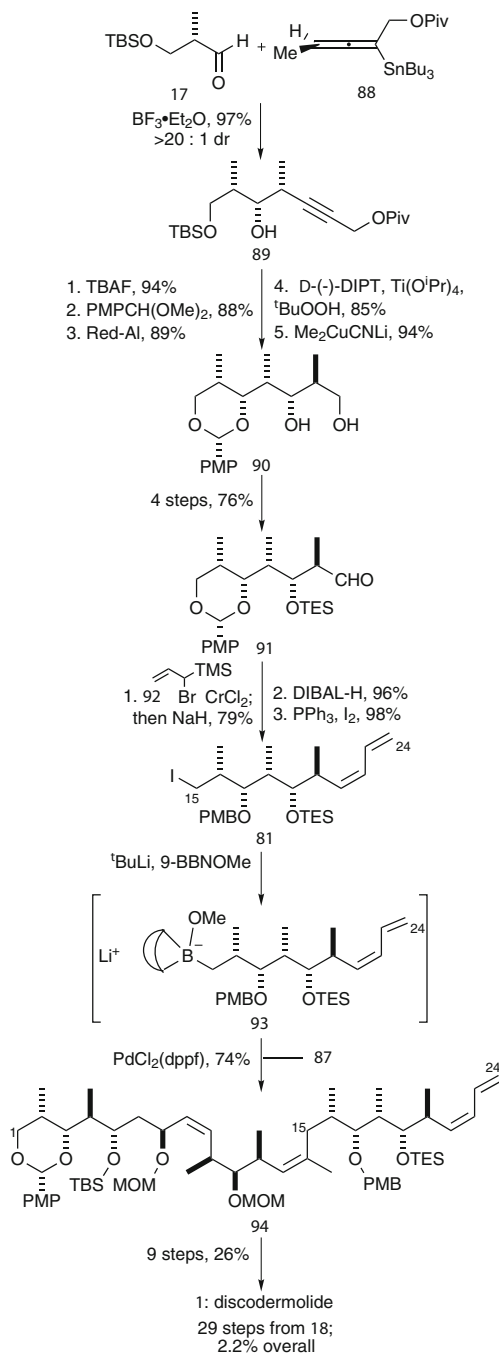
In the synthesis of the C15–C24 subunit **81**, Marshall utilized the Lewis-acid promoted addition of the allenylstannane **88** to aldehyde **17** to configure the *syn* stereotriad in **89** (Scheme 20) [128, 129]. A five-step sequence was then required to configure the C19–C20 stereocentres, involving hydroalumination, Sharpless epoxidation and epoxide opening with lithium dimethylcyanocuprate. Conversion of **90** into aldehyde **91** was followed by (*Z*)-diene installation using the Paterson and Schlapbach protocol [75], involving sequential Nozaki–Hiyama addition of allylbromosilane **92** and Peterson-type elimination. Following manipulation of the C15-terminus, iodide **81** was transformed into the intermediate C15–C24 boronate **93** for the Suzuki cross-coupling reaction with **87**, thus assembling the C1–C24 intermediate **94**. A further nine steps involving a series of protecting group manipu-



Scheme 19 Marshall's synthesis of the C1–C14 intermediate

lations and oxidation state adjustments then completed Marshall's synthesis of discodermolide in 2.2% overall yield over 29 steps (longest linear sequence).

The Marshall synthesis clearly demonstrated both the versatility of allenyl metal methodology for the preparation of polypropionate arrays and the utility of the Suzuki cross-coupling in complex fragment assembly.

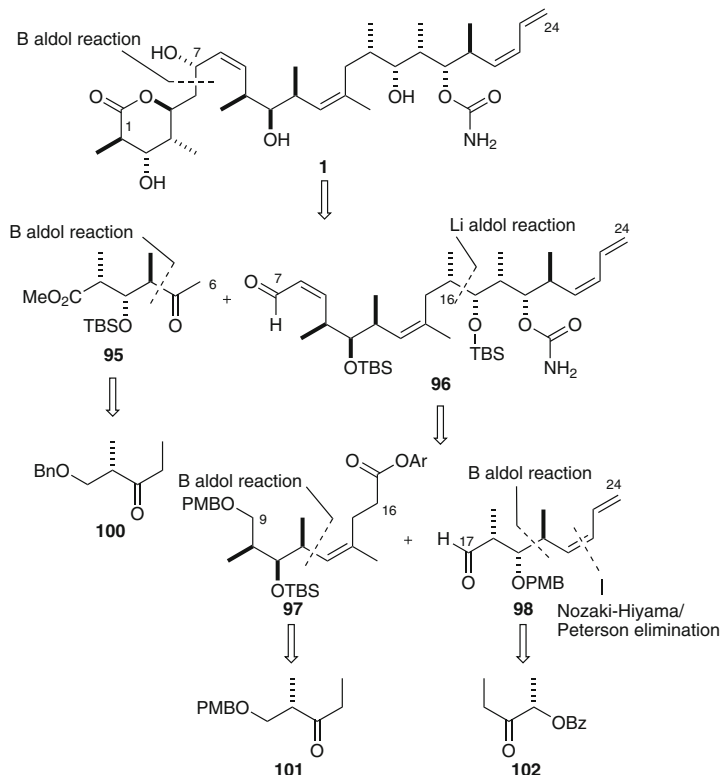
**Scheme 20** Marshall's synthesis of the C15–C24 subunit and completion of discodermolide

2.5 Paterson Total Synthesis

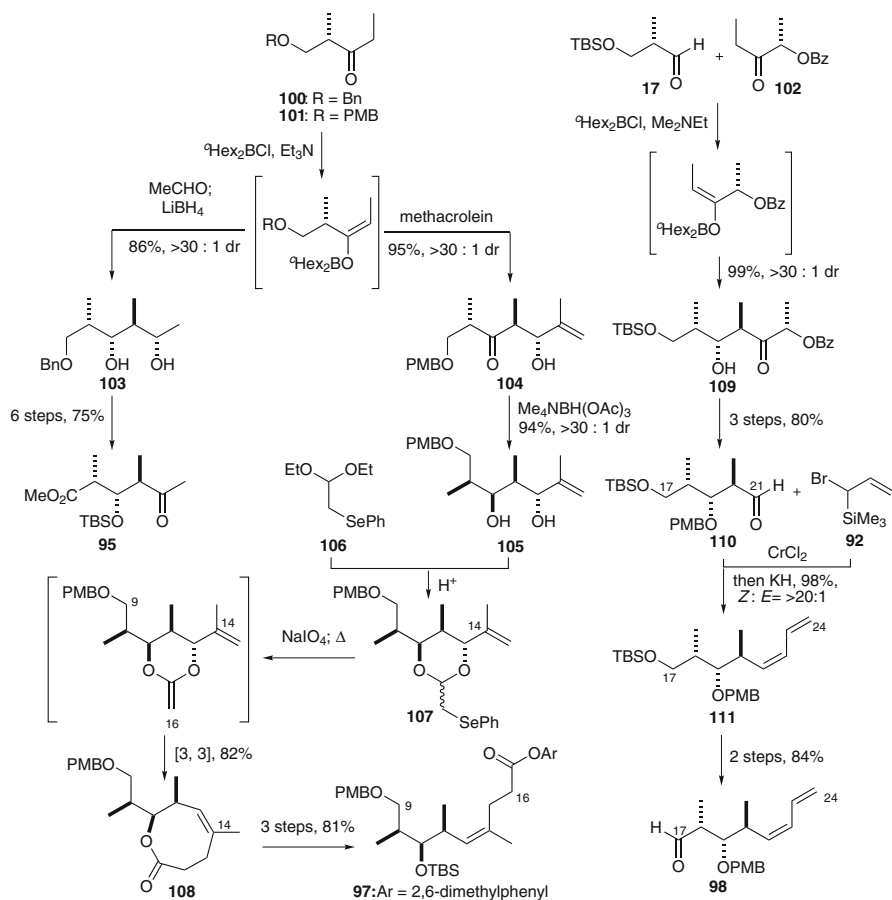
2.5.1 First Generation (2000)

In 2000, Paterson and co-workers reported their first-generation synthesis of discodermolide [55–57]. As shown in Scheme 21, their novel construction of the carbon skeleton of discodermolide relied on an ambitious boron aldol coupling reaction at C6–C7 between methyl ketone **95** and the advanced (*Z*)-enal **96**, and an equally challenging lithium-mediated aldol reaction at C16–C17 between aryl ester **97** and aldehyde **98**, thus installing three new stereogenic centres in the fragment union steps. In turn, the *anti* aldol reactions of the respective chiral ethyl ketones **100–102** were used to configure the stereochemical motifs in the three subunits **95** (C1–C6) [130], **97** (C9–C16) [131] and **98** (C17–C24) [131–138] (see [139] for a review). In addressing the installation of the trisubstituted (*Z*)-alkene in **97**, the application of Holmes' Claisen rearrangement methodology provided a further novel solution [140–144], which also introduced the correct oxidation state for the planned C16–C17 aldol coupling.

As outlined in Scheme 22, the synthesis of the C1–C6 subunit **95** commenced with the *anti* aldol reaction of the ethyl ketone **100**, prepared in three steps from Roche ester **18**, and acetaldehyde, with in situ reduction to give diol **103** (>30:1dr) [130, 132–136, 145, 146]. Completion of **103** then required a series of protecting group manipulations



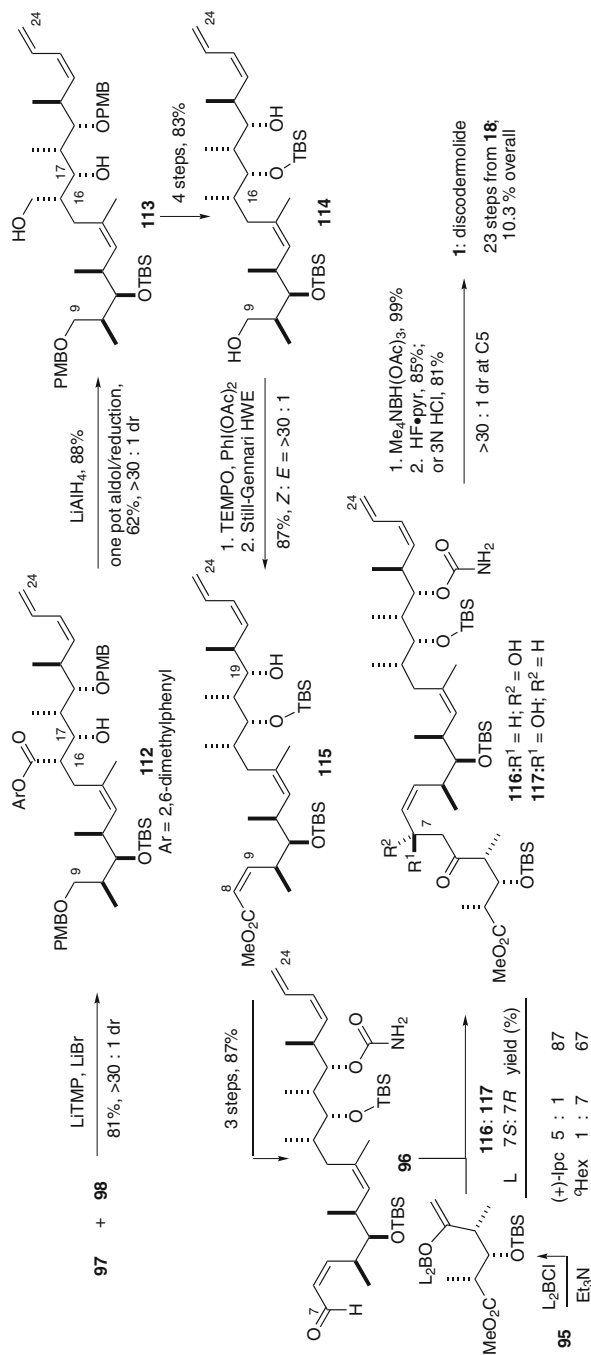
Scheme 21 Paterson's first-generation strategy



Scheme 22 Paterson's synthesis of the C1–C6, C9–C16 and C17–C24 subunits

and oxidation state adjustments. The synthesis of the C9–C16 aryl ester **97** began with the *anti* aldol reaction of ethyl ketone **101** and methacrolein to provide **104** (>30:1dr) [130, 132–136]. A 1,3-*anti* reduction provided diol **105** (>30:1dr) [114], which then underwent transacetalisation with **106**. Following the Holmes protocol [140–144], oxidation of **107** followed by thermal selenoxide elimination gave the transient ketene acetal which underwent Claisen [6, 6] rearrangement to afford the 8-membered lactone **108**, introducing the trisubstituted C13–C14 (*Z*)-alkene cleanly. Opening of **108**, esterification and TBS protection then completed **97**. The synthesis of the C17–C24 aldehyde **98** began with an *anti* aldol reaction between the lactate-derived ketone **102** and the aldehyde **17** to provide **109** (>30:1dr) [131, 137, 138]. Transformation to aldehyde **110** was followed by the Paterson and Schlaapbach diene installation, involving sequential Nozaki-Hiyama allylation with bromide **92** and Peterson elimination [75]. Conversion of **111** into aldehyde **98** then paved the way for the first of the key fragment unions.

As shown in Scheme 23, the lithium-mediated *anti* aldol reaction of the aryl ester **97** and aldehyde **98** gave the expected Felkin-Anh adduct **112** (30:1dr) [147, 148].



Scheme 23 Paterson's subunit assembly and completion of discodermolide

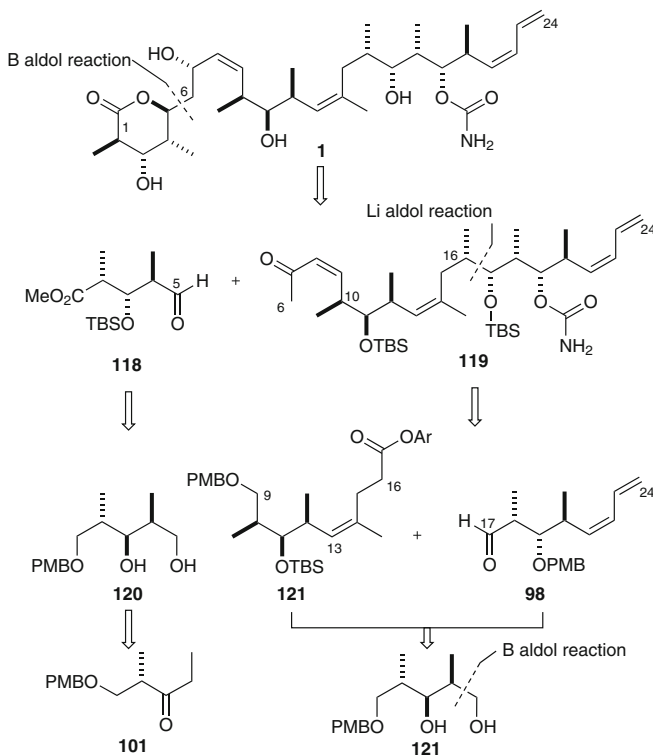
Following ester reduction, either in situ or upon isolation of **112**, the superfluous oxygen functionality at C16 in diol **113** was removed and converted into intermediate **114** in four steps. Selective primary oxidation with TEMPO [149], followed by a Still-Gennari HWE olefination [106] installed the C8–C9 (*Z*)-olefin in **115** (*Z:E* \Rightarrow 30:1). Transformation into enal **96** required three further steps, prior to the final C6–C7 aldol coupling. Considerable effort was required to secure the desired adduct **116** bearing the correct C7 configuration [56, 57]. Using the achiral boron reagent *c*Hex₂BCl for enolization of **95** gave the undesired (*7R*)-adduct **117** (7:1dr). This unprecedented selectivity arose from high levels of remote 1,4-stereinduction imparted by the aldehyde component. In order to overturn the π -facial bias of aldehyde **96**, the chiral (+)-Ipc₂BCl reagent was employed and the desired (*7S*)-adduct **116** was now obtained with 5:1 dr (see [139] for a review) [150–152]. An Evans 1,3-*anti* reduction of **116** introduced the final stereogenic centre at C5 (>30:1dr) [114], which following acid-mediated desilylation and δ -lactonization gave discodermolide, completing the Paterson group's first-generation synthesis in 10.3% yield over 23 steps (longest linear sequence).

The Paterson first-generation synthesis of discodermolide provides a clear demonstration of the utility of complex boron aldol reactions in the context of polyketide natural product synthesis. Recently, Paton and Goodman reported theoretical DFT studies of related boron aldol transition states to rationalise the very high degrees of stereoselectivity obtained in these powerful reactions [153]. In contrast to previous syntheses, essentially complete control was now achieved over the double bond geometries and the only step proceeding with less than optimal stereocontrol was the final mismatched aldol coupling. However, it is notable that the Novartis process group chose to adopt the key C6–C7 aldol disconnection in their large-scale synthesis of discodermolide for clinical trials (see Sect. 2.8).

2.5.2 Second Generation (2003)

In 2003, Paterson and co-workers reported a second-generation strategy for the synthesis of discodermolide, which aimed to eliminate the use of all chiral reagents and auxiliaries, and reduce the total number of synthetic steps (Scheme 24) [58, 59]. These specific aims were achieved by employing an unprecedented aldol coupling at C5–C6 between C1–C5 aldehyde **118** and the advanced C6–C24 methyl ketone **119** and utilising diol **120** as a common precursor for the synthesis of the three subunits **118**, **121** (C9–C16) and **98** (C17–C24).

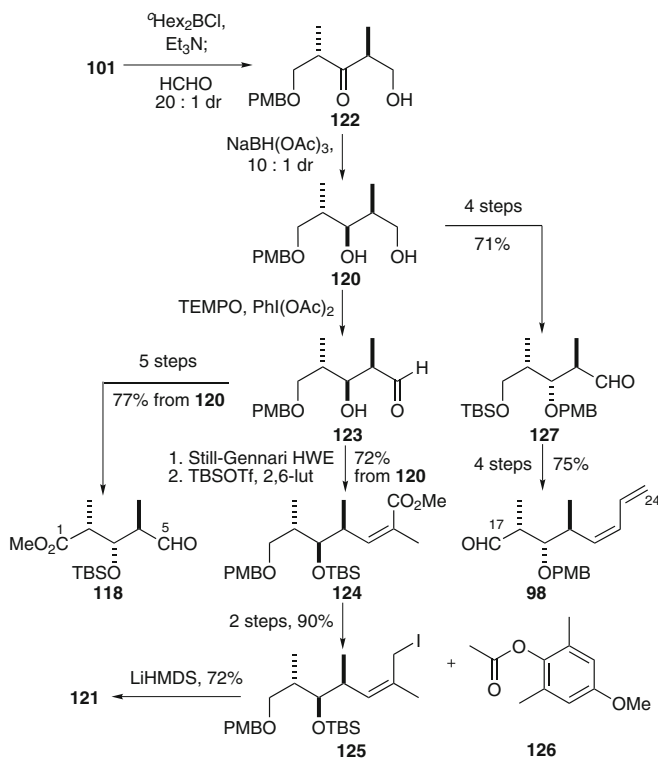
The common precursor **120** was prepared in two steps from ethyl ketone **101** on a multigram scale (Scheme 25), where the 1,3-*anti* methyl groups were configured by a boron aldol reaction with formaldehyde (20:1dr) [130, 132–136]. Aldol adduct **122** then underwent a hydroxyl-directed reduction to provide diol **120** (10:1dr). The C1–C5 subunit **118** was prepared in six steps from diol **120**, starting with the selective TEMPO oxidation of the C1-OH to give aldehyde **123**, and five further steps involving oxidation state adjustments and protecting group manipulations followed. Aldehyde **123** was also used in the five-step preparation of the C9–C16 subunit **121**.



Scheme 24 Paterson's second-generation strategy

The trisubstituted (*Z*)-olefin was introduced by Still-Gennari HWE olefination, as preceded by Schreiber [43, 44, 106], and following silyl protection provided **124**. Conversion into the iodide **125** was followed by alkylation with the lithium enolate of aryl ester **126**, to complete the C9–C16 subunit **121**. The synthesis of the C17–C24 subunit **98** from **120** began with a four-step sequence involving protecting group manipulations and oxidation at C21 to provide aldehyde **127**, converging with the earlier route to **98** [55–57].

As outlined in Scheme **26**, assembly of the subunits began with the lithium-mediated aldol coupling of **121** and **98** to provide **129** (6:1dr) [147, 148], which was converted into the diol **114**, following the first-generation route [55–57]. Primary oxidation of **114** and modified Still-Gennari olefination introduced the (*Z*)-enone moiety in **119** (*Z*:*E* = 12:1) [106, 154]. The boron aldol reaction of methyl ketone **119** and aldehyde **118** gave the desired (*5S*)-adduct **130** with 20:1dr, arising from long-range 1,6-asymmetric induction from the remote C10 γ -stereocentre in the ketone component. Acid-promoted δ -lactonisation of **130**, K-Selectride reduction of the C7 ketone (>30:1dr) [46–48] and global deprotection then completed the second-generation synthesis of discodermolide in 5.1% overall yield, with 24 steps in the longest linear sequence.

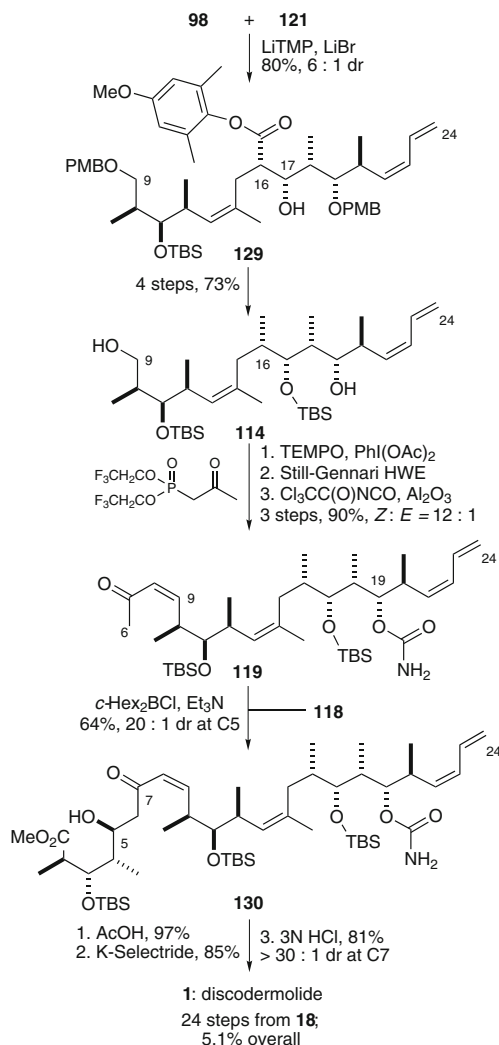


Scheme 25 Paterson's synthesis of C1–C5, C9–C16 and C17–C24 subunits from common precursor diol

The Paterson second-generation approach substantially reduced the total number of steps required to complete discodermolide. Notably, the use of chiral reagents and auxiliaries was completely eliminated, relying solely on substrate control to configure all the remaining stereocentres from the ubiquitous Roche ester (**18**), achieving a more cost-effective route.

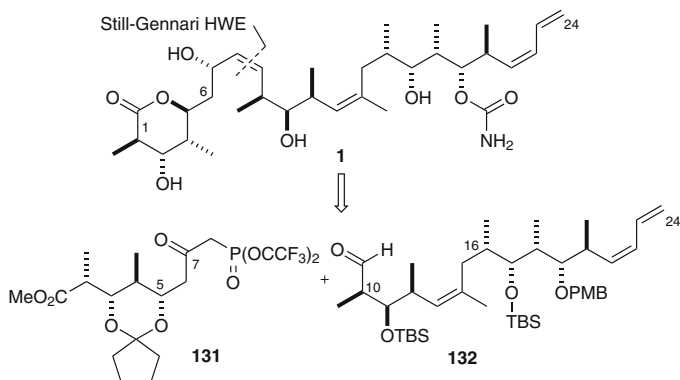
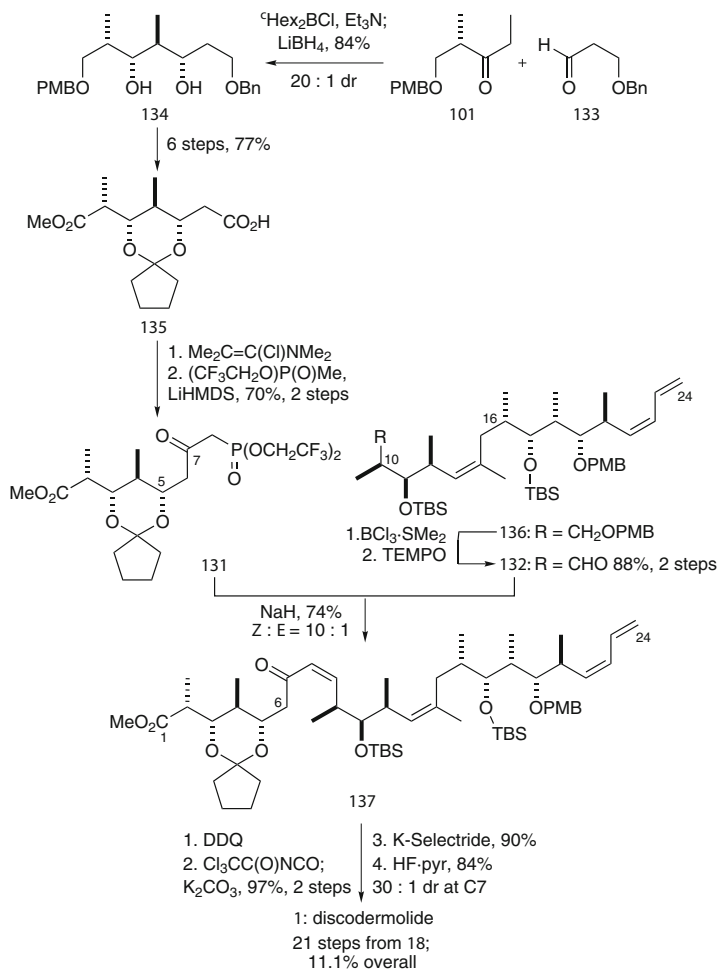
2.5.3 Third Generation (2004)

In 2004, the Paterson group implemented a further revision to their strategy designed to overcome the perceived technical difficulties of performing late-stage boron aldol couplings on an industrial scale (Scheme 27) [60, 61]. Building on the experience already gained and their contemporary synthesis of dictyostatin (**2**), a third-generation approach to discodermolide involved the application of a Still-Gennari-type HWE olefination in the final fragment coupling step using the highly functionalized C1–C8 β -ketophosphonate **131** and the C9–C24 aldehyde **132**.



Scheme 26 Paterson's second generation subunit assembly and completion of discodermolide

As outlined in Scheme 28, the synthesis of the β -ketophosphonate **131** began with a one-pot *anti*-aldol/reduction step between ethyl ketone **101** and aldehyde **133**, giving the 1,3-syn diol **134** (>30:1dr) [130, 132–136, 145, 146]. The diol **134** was then converted into the carboxylic acid **135** in six steps. Completion of the subunit **131** required conversion into the acid chloride and reaction with the lithium anion of methyl-(di-1,1,1-trifluoroethyl)-phosphonate. The C9–C24 aldehyde **132** was prepared in two steps from **136**, an intermediate from previous routes [55–58]. The Still-Gennari-type coupling of **131** and **132** was readily achieved via treatment with

**Scheme 27** Paterson's third-generation strategy**Scheme 28** Paterson's synthesis of C1-C8 phosphonate and completion of third-generation synthesis

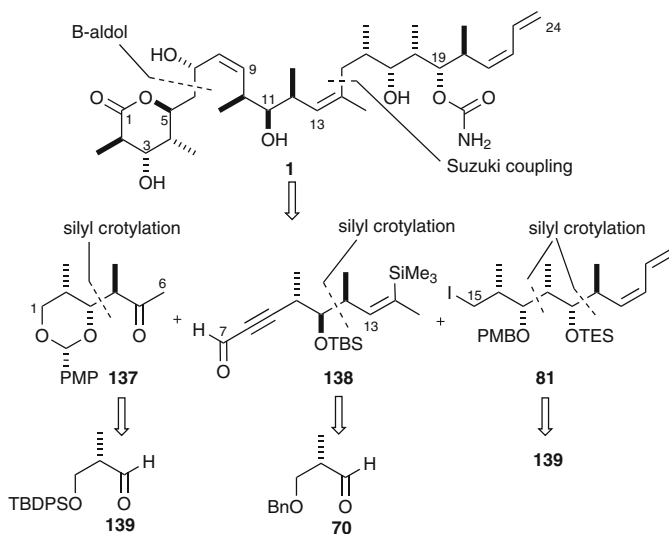
NaH to give the advanced enone **137** (*Z:E* = 10:1). A further four steps were then required to complete the third-generation synthesis, beginning with C19 carbamate installation, followed by K-Selectride reduction to introduce the requisite (7*S*)-stereocentre. Finally, global deprotection with concomitant δ -lactonisation gave discodermolide (**1**) in 11.1% overall yield over 21 steps (longest linear sequence).

In summary, the Paterson group's third-generation synthesis demonstrated the versatility of the Still-Gennari HWE coupling of advanced polypropionate subunits. This revised endgame gave improved levels of efficiency and, importantly, the overall linear sequence was shortened with increased yields. The experimentally undemanding conditions of the Still-Gennari-type HWE coupling protocol offers distinct advantages over previous routes using boron aldol reactions, offering a viable alternative for industrial scale-up.

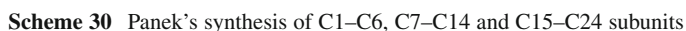
2.6 Panek Total Synthesis

Panek and co-workers reported their synthesis of discodermolide in 2005 [62, 63], relying on the application of their crotylsilane methodology for the synthesis of polypropionate motifs [155, 156] (see [157] for a review) [158, 159, 182]. Their strategy involved key bond disconnections at C6–C7 and C14–C15, based on an aldol coupling and the established Suzuki cross-coupling respectively, employing the key subunits **137** (C1–C6), **138** (C7–C14) and **81** (C15–C24) (Scheme 29).

As outlined in Scheme 30, the synthesis of the C1–C6 subunit **137** began with the crotylation of aldehyde **139** with the (*S*)-allylsilane **140**, which following silyl depro-



Scheme 29 Panek's synthetic strategy



tection gave diol **141** (dr > 30:1) [81, 168, 170, 171] (see [157] for a review). Subsequent anisylidene acetal formation and ozonolysis completed **137**. The (*S*)-crotylsilane **142** was used as the starting point for the synthesis of the C7–C14 subunit with its addition to aldehyde **70**. A four-step sequence on **143** was then used to access the silylacetylene **144**, which upon treatment with Schwartz's reagent [160, 161] and quenching with iodine gave (*Z*)-iodovinylsilane **145**. A palladium-mediated

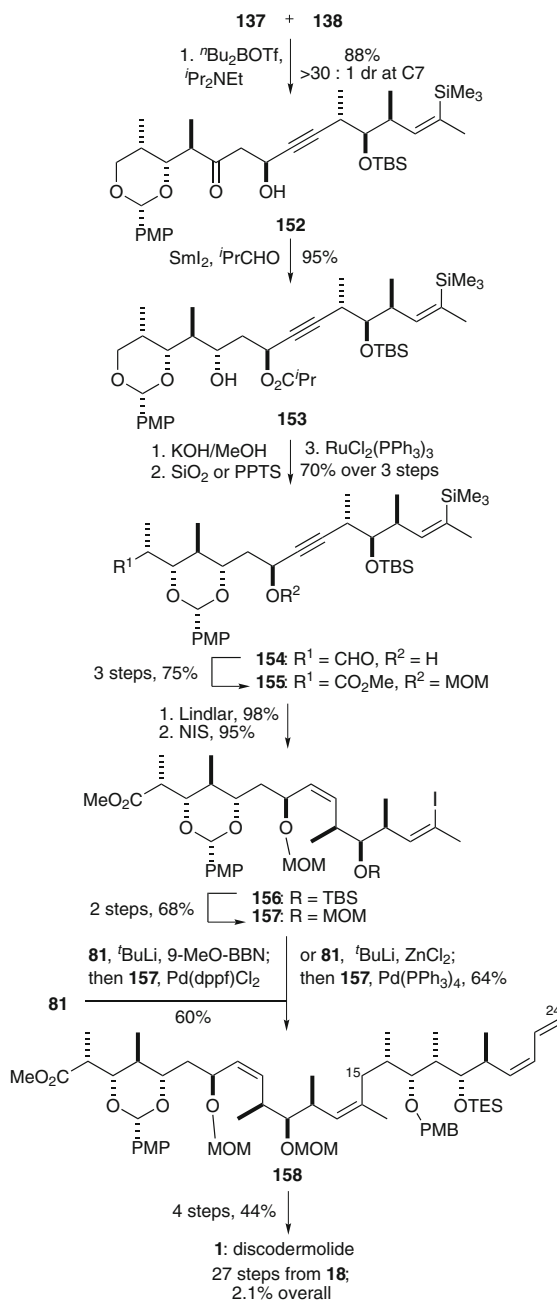
coupling of **145** with methylzinc chloride gave the (*Z*)-vinylsilane **146** exclusively, providing a further solution for the installation of the C13–C14 trisubstituted olefin. The subunit **138** was then completed by the Corey-Fuchs olefination at C9, treatment of the intermediate vinyl dibromide with BuLi and quenching with ethyl formate. The synthesis of the C17–C24 subunit **81** started with the crotylation of aldehyde **139** with (*R*)-crotylsilane **147** to configure the all-*syn* stereotriad in **148**. Conversion into the aldehyde **149** was followed by a second crotylation, now with (*S*)-crotylsilane **142**, to configure the C19–C20 stereocentres in **150**, which was then transformed into the aldehyde **151** in four steps. Treatment of **151** with a Roush-type allylboronate reagent and subsequent Peterson elimination selectively introduced the terminal (*Z*)-diene [51, 52, 125], which was readily transformed into iodide **81**.

As outlined in Scheme 31, Panek's assembly of subunits began with the boron-mediated aldol reaction of ketone **137** and aldehyde **138**, which gave the expected 1,4-*syn*-1,5-*anti* aldol product **152** [162, 163]. An Evans-Tischenko reduction efficiently introduced the C5-stereocentre in **153** [164]. Methanolysis, acid-mediated migration of the PMP acetal and primary oxidation with Oshima's reagent [165] gave aldehyde **154**, which was converted into **155** in three steps. Lindlar reduction of the C8–C9 alkyne, and conversion of the C14-vinyl silane into the vinyl iodide **156**, then set the stage for the C14–C15 bond formation. The success of both Suzuki- and Negishi-type couplings required exchange of the protecting group at C13 from TBS in **156** to MOM in **157**, which then underwent cross-coupling with iodide **81** to provide **158** [53, 54, 105, 116]. The completion of discodermolide from **159** then required an additional four steps. Overall, Panek's synthesis proceeded in 2.1% yield based on 27 steps (longest linear sequence).

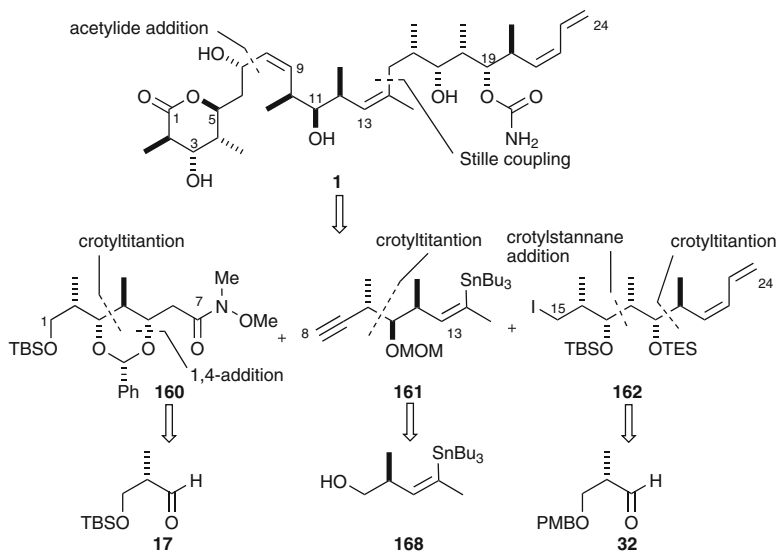
2.7 Ardisson Total Synthesis

In 2007, Betzer, Ardisson and co-workers reported their synthesis of discodermolide [64] following the Marshall disconnection strategy of C7–C8 acetylide addition and Suzuki cross-coupling at C14–C15 (Scheme 32) [53, 54]. The synthesis of the key subunits **160** (C1–C7), **161** (C8–C14) and **162** (C15–C24) demonstrated the versatility of the Hoppe crotyltitanation reaction [166–169] in the synthesis of polypropionate motifs, using the incorporated (*Z*)-*O*-enecarbamate to configure the requisite alkene substitution patterns [170, 171].

As shown in Scheme 33, the synthesis of the C1–C7 amide **160** began with a Hoppe crotyltitanation reaction between the aldehyde **17** and the (*R*)-crotyltitanium **163**, prepared in situ (crotyl diisopropylcarbamate with *s*BuLi/(–)-sparteine/Ti(O*i*Pr)₄), to give *O*-enecarbamate **164** (>30:1dr) [166–169]. Ozonolysis and HWE chain extension was followed by an Evans-Prunet 1,4-addition to install the C5-stereocentre to complete **160** [103]. The synthesis of the C8–C14 subunit **161** started with an elegant installation of the C13–C14 (*Z*)-olefin. Deprotonation of the dihydrofuran **165**, available in three steps from bromo alcohol **166**, with *t*BuLi and transmetallation with Me₂CuLi–LiCN, and subsequent 1,2-cuprate transfer gave the



Scheme 31 Panek's subunit assembly and completion of discodermolide



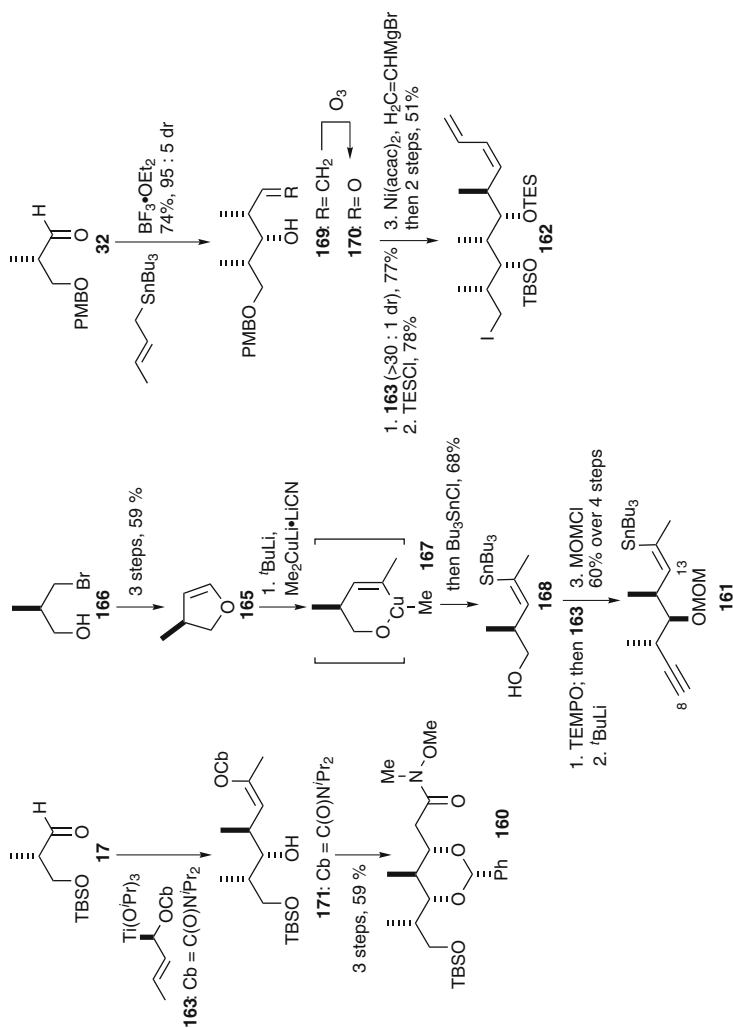
Scheme 32 Ardisson's synthetic strategy

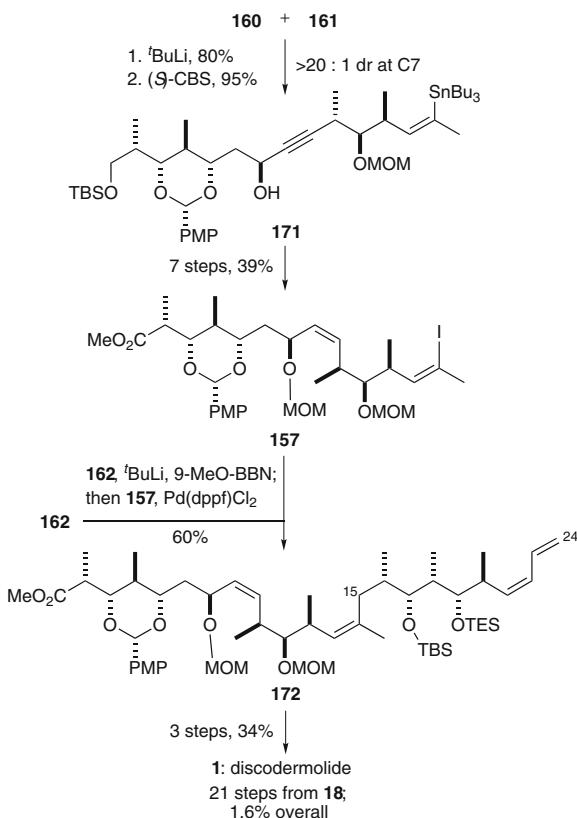
intermediate **167**, which was trapped with tributyltin chloride to provide the (*Z*)-vinyl stannane **168** exclusively [172–175]. Oxidation of **168** was followed by a second Hoppe reaction with **163** to give the intermediate (*Z*)-*O*-enecarbamate, which underwent Fritsch-Buttenberg-Wiechell rearrangement to give, after MOM protection, alkyne **161** (see [176] for review) [177]. The synthesis of the C15–C24 subunit **162** commenced with the diastereoselective crotylation of aldehyde **32** with (*E*)-crotylstannane to give **169**. Conversion into aldehyde **170** was followed by a third crotylation reaction with **163** (>30:1 dr). A four-step sequence was then required to complete **162**, in which the terminal (*Z*)-diene was installed via a nickel-catalysed cross coupling of the C22-carbamate with vinylmagnesium bromide.

The assembly of the subunits began with the addition of the lithium anion of acetylene **161** to Weinreb amide **160**, followed by CBS reduction to give **171** installing the C7 stereocentre with > 20:1 dr (Scheme 34) [178]. Following elaboration to vinyl iodide **157**, an intermediate shared with the Panek route [62, 63], Suzuki cross-coupling with the boronate derived from iodide **162** gave the advanced C1–C24 intermediate **172**, which following a three-step sequence provided discodermolide in 1.6% yield over 21 steps (longest linear sequence).

2.8 Novartis Process Chemistry Group Synthesis

Early preclinical development of discodermolide had shown its clear potential as a new generation anticancer agent for the treatment of a range of multidrug-resistant human cancers. This attracted the attention of Novartis Pharma AG, who with a

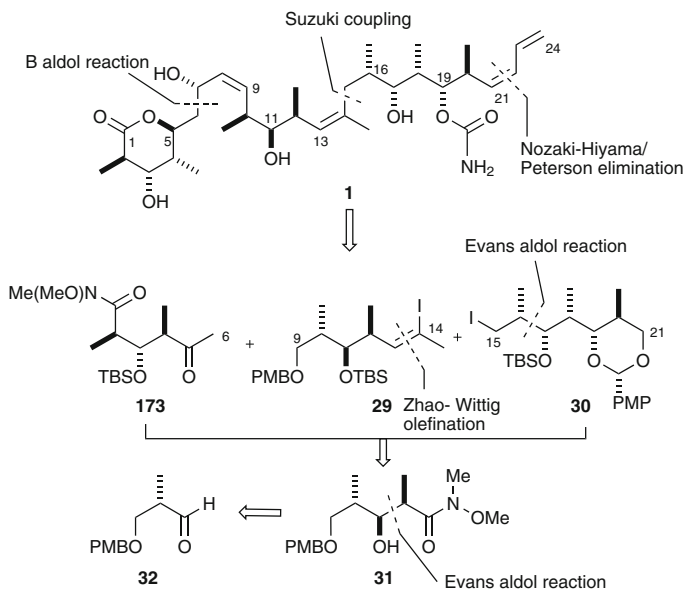
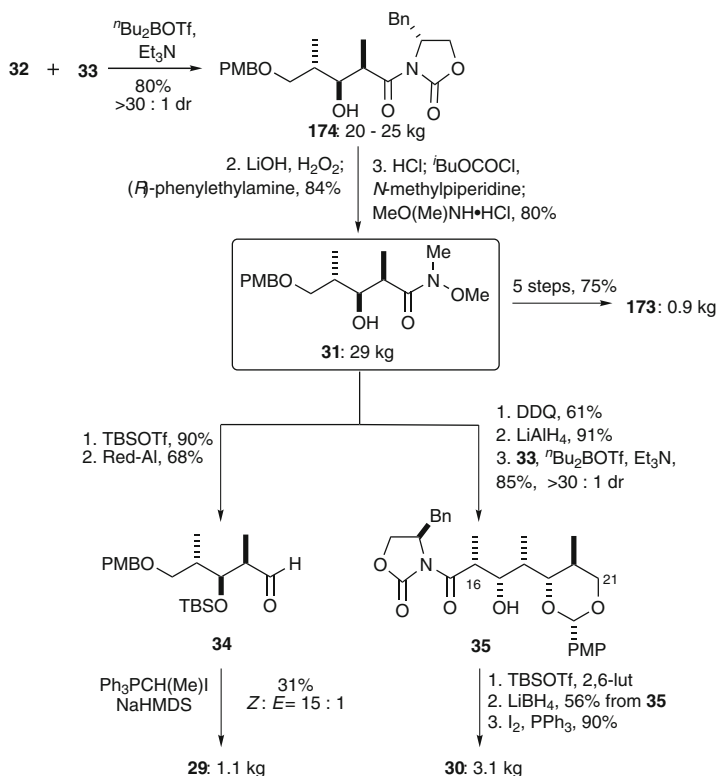
**Scheme 33** Ardisson's synthesis of C1–C7, C8–C14 and C15–C24 subunits



Scheme 34 Ardisson's subunit assembly and completion of discodermolide

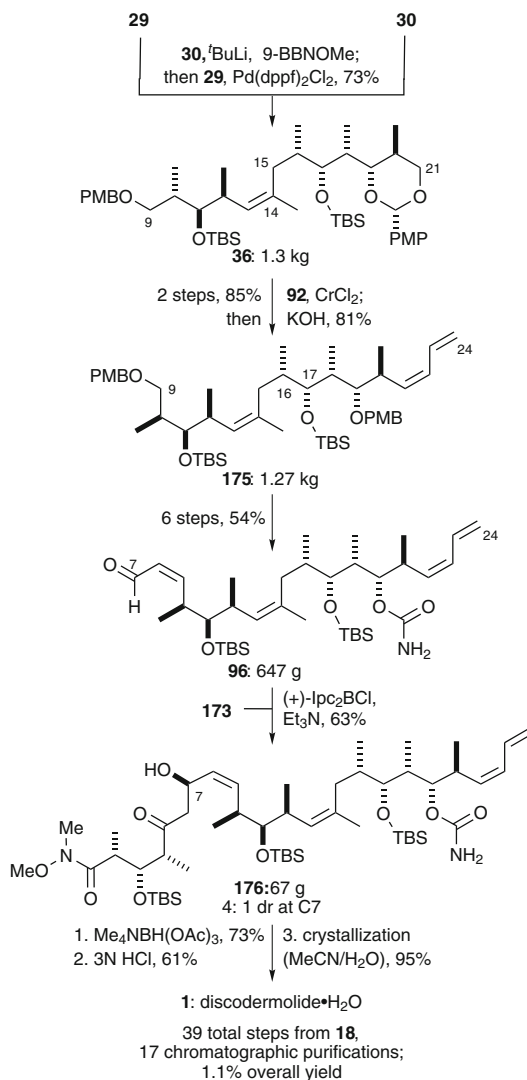
license agreement from the Harbor Branch Oceanographic Institution, took on the task of progressing discodermolide into clinical trials. This required a practical synthetic solution [65–69, 90, 92, 95], as eco-harvesting the rare natural source was clearly not an option, either economically or ecologically. Rising to this challenge, the Novartis Process Chemistry group in Basel led by Mickel reported in 2004 the synthesis of 64 g of discodermolide.[65–69]. Following careful consideration of the successful approaches to discodermolide at the time, Mickel and co-workers adopted a hybrid synthesis incorporating features of the Smith [45, 46] and Paterson [55–57] routes (Sects. 2.2 and 2.5, respectively), providing valuable insights into the complexities of performing a multistep “academic” synthesis in an industrial setting. As outlined in Scheme 35, the Novartis strategy opted for Paterson's aldol disconnection at C6–C7 and the Smith/Marshall cross-coupling at C14–C15. In turn, the three key subunits **173** (C1–C6), **29** (C9–C14) and **30** (C15–C24) would be accessed on a kilogram-scale from Smith's common precursor **31** [46–48].

As shown in Scheme 36, the Novartis group's large-scale (20–25 kg) preparation of Smith's common precursor **31** began with the established Evans aldol reaction between the Roche ester-derived aldehyde **32** and the propionimide **33** [65].

**Scheme 35** Novartis synthetic strategy**Scheme 36** Novartis large-scale synthesis of C1–C6, C9–C14 and C15–C21 subunits

Transformation of **174** into the common precursor **31** could not be achieved directly due to safety considerations regarding the use of Me_3Al on pilot plant scale. Thus, hydrolysis of **174** and isolation of the intermediate acid salt, was followed by the formation of a mixed anhydride and subsequent amide formation to provide 29kg of **31** [179, 180]. Having achieved access to the common precursor, the synthesis of the C1–C6 subunit **142** was completed in five steps in 66% yield on scales of several kilograms, only requiring chromatographic purification at the final stage [66]. The synthesis of the C9–C14 subunit **31** essentially followed an analogous route to Smith [46–48, 66]. Following TBS protection of **31**, Red-Al was used in preference to DIBAL-H for the reduction to aldehyde **34**. At this stage, introduction of the C13–C14 (Z)-vinyl iodide was required and, as expected from the work of Smith and Marshall, the Zhao-Wittig olefination gave only moderate yields of **29**, limiting the scale of the reaction to a maximum of 2.5kg substrate. The synthesis of the C15–C21 subunit **30** followed the Smith route [46–48, 67], beginning with the conversion of **31** into the intermediate aldehyde for the Evans aldol reaction with **33**. In order to minimise the formation of by-products in this reaction, it was necessary to maintain the reaction below -10°C at all times and required a “rapid workup and isolation” to prevent epimerization at C16 which was readily observed at ambient temperatures [67]. The problems associated with epimerisation were negated by the subsequent silyl protection of **35**. However, the reductive removal of the auxiliary with LiBH_4 led to the formation of numerous by-products requiring careful chromatographic purification of ca. 1-kg batches of crude material, prior to the formation of iodide **30**.

As outlined in Scheme 37, the Novartis assembly of discodermolide began with the Marshall Suzuki-type cross-coupling of vinyl iodide **29** and iodide **30** to give **36** on a kilogram scale [68]. At this point, the crossover of routes required the introduction of the terminal (Z)-diene to give the Paterson intermediate **175** [55–57]. Following an analogous six-step sequence to that reported by the Paterson group, 810g of the C7–C24 (Z)-enal **96** was prepared from **175**. Notably, this only required two chromatographic purifications – after the Still-Gennari HWE reaction to introduce the (Z)-olefin at C8–C9 and following the final oxidation step. With substantial quantities of **96** available, the reagent-controlled boron aldol coupling with ketone **173** posed the largest challenge of the entire scale-up campaign [55–57, 69, 181]. In order to obtain reproducible yields of the desired aldol adduct **176**, a number of limiting factors were identified, namely reagent quality and handling, work-up and isolation procedures. It was found that a commercial solution of (+)- Ipc_2BCl in hexane proved to be more reliable in terms of quality than the highly hygroscopic solid form and also conveniently negated the issue of handling the solid reagent. It was found that an oxidative work-up procedure should be avoided in favour of the direct purification of the crude product mixture by reverse phase chromatography, leading to the formation of **176** in 50–55% yield. In contrast, the introduction of the C7-stereocentre by Evans-Saksena reduction and global deprotection proved uneventful. Finally, reverse phase chromatography and crystallisation provided a 64-g batch of pure discodermolide monohydrate [69].



Scheme 37 Novartis fragment assembly and completion of discodermolide

The Novartis Process Chemistry group's preparation of discodermolide represents a landmark in the industrial synthesis of complex natural products and pharmaceutical development. Having taken the bold decision to pursue the clinical development of discodermolide under tight time constraints, they met the challenge of combining the approaches of Smith and Paterson and delivering sufficient quantities of active pharmaceutical ingredient to enable clinical trials.

Table1 Comparison of the completed syntheses of discodermolide (1993–2007)

Research group	Year	Linear sequence	Overall yield(%)	Substrate-controlled stereocentres ^a	Reagent-controlled stereocentres ^b	Chiral pool stereocentres ^c
Schreiber	1993	24	4.3	4	6	3
Smith I	1995	28	2.2	1	8	4
Myles ^d	1997	22	1.1	5	5	3
Marshall	1998	29	2.2	2	8	3
Smith II	1999	24	6.0	2	8	3
Paterson I	2000	23	10.3	7	3	3
Paterson II	2003	24	5.1	10	0	3
Smith III	2003	24	1.9	2	8	3
Novartis	2004	25	1.1	1	9	3
Paterson III	2004	21	11.1	10	0	3
Panek	2005	27	2.1	2	8	3
Smith IV	2005	17	9.0	2	8	3
Ardisson	2007	21	1.6	3	7	3

^aStereocentres configured by substrate-controlled reactions^bStereocentres configured by reagent–auxiliary-controlled reactions^cStereocentres accessed from chiral pool starting materials^dData from Myles' full disclosure in 2003 [52]

3 Summary

The various synthetic approaches developed to date have served to eliminate the supply problem for discodermolide, enabling extensive biological evaluation and early stage clinical development of this remarkable microtubule-stabilising anticancer agent. Discodermolide has inspired many creative and elegant total syntheses based on the application of contemporary methods of substrate and reagent based stereo-control; these approaches are summarized chronologically in Table1. Importantly, this shows that natural products with challenging molecular architectures can be accessed synthetically in an efficient and timely manner, and further underlines their resurgence as serious candidates for drug development [8]. Thanks to the power of modern organic synthesis, one can contemplate the practical synthesis of other such complex natural products where the natural supply is insufficient for detailed biological evaluation, let alone potential clinical application.

References

1. Blunt JW, Copp BR, Hu WP, Munro MHG, Northcote PT, Prinsep MR (2007) *Nat Prod Rep* 24:31
2. Blunt JW, Copp BR, Munro MHG, Northcote PT, Prinsep MR (2006) *Nat Prod Rep* 23:26
3. Blunt JW, Copp BR, Munro MHG, Northcote PT, Prinsep MR (2005) *Nat Prod Rep* 22:15
4. Blunt JW, Copp BR, Munro MHG, Northcote PT, Prinsep MR (2003) *Nat Prod Rep* 20:1
5. Koehn FE, Carter GT (2005) *Nat Rev Drug Discov* 4:206
6. Butler MS (2005) *Nat Prod Rep* 22:162

7. Newman DJ, Cragg GM (2007) *J Nat Prod* 70:461
8. Paterson I, Anderson EA (2005) *Science* 310:451
9. Hamann MT, Hill R, Roggo S (2007) *Chimia* 61:313
10. Paterson I, Florence GJ (2003) *Eur J Org Chem* 2193
11. Mickel SJ (2007) *Pure Appl Chem* 79:685
12. Kalesse M (2000) *ChemBioChem* 1:171
13. Smith AB, Freeze BP (2008) *Tetrahedron* 64:261
14. Paterson I, Yeung KS (2005) *Chem Rev* 105:4237
15. Altmann KH, Gertsch J (2007) *Nat Prod Rep* 24:327
16. Kuppens IELM (2006) *Curr Clin Pharmacol* 1:57
17. Gunasekera SP, Gunasekera M, Longley RE, Schulte GK (1990) *J Org Chem* 55:4912; correction (1991) *J Org Chem* 56:1346
18. Gunasekera SP, Paul GK, Longley RE, Isbrucker RA, Pomponi SA (2002) *J Nat Prod* 65:1643
19. Smith AB, LaMarche MJ, Falcone-Hindley M (2001) *Org Lett* 3:695
20. Longley RE, Caddigan D, Harmody D, Gunasekera M, Gunasekera SP (1991) *Transplantation* 52:650
21. Longley RE, Caddigan D, Harmody D, Gunasekera M, Gunasekera SP (1991) *Transplantation* 52:656
22. ter Haar E, Kowalski RJ, Hamel E, Lin CM, Longley RE, Gunasekera SP, Rosenkranz HS, Day BW (1996) *Biochemistry* 35:243
23. Horwitz SB, Cohen D, Rao S, Shen HJ, Yang CP (1993) *J Natl Cancer Inst* 15:55
24. Bollag DM, McQueney PA, Zhu J, Hensens O, Koupal L, Liesch J, Goetz M, Lazarides E, Woods CM (1995) *Cancer Res* 55:2325
25. D'Ambrosio M, Guerriero A, Pietra F (1987) *Helv Chim Acta* 70:2019
26. Lindel T, Jensen PR, Fencial W, Long BH, Casazza AM, Carboni J, Fairchild CR (1997) *J Am Chem Soc* 119:8744
27. Mooberry SL, Tien G, Hernez AH, Plubrukarn A, Davidson BS (1999) *Cancer Res* 59:653
28. Sato B, Nakajima H, Hori Y, Hashimoto S, Terano H (2000) *J Antibiot* 53:204
29. Hood KA, West LM, Rouwe B, Northcote PT, Berridge MV, Wakefield J, Miller JH (2002) *Cancer Res* 62:3356
30. Pettit GR, Chicacz ZA, Gao F, Boyd MR, Schmidt JM (1994) *J Chem Soc Chem Commun* 1111
31. Isbrucker RA, Cummins J, Pomponi SA, Longley RE, Wright AE (2006) *Biochem Pharmacol* 66:75
32. Paterson I, Britton R, Delgado O, Wright AE (2004) *Chem Commun* 632
33. Boven E, Venema-Gaberscek E, Erkelens CA, Bissery MC, Pinedo HM (1993) *Ann Oncol* 4:321
34. Kowalski RJ, Giannakakou P, Gunasekera SP, Longley RE, Day BW, Hamel E (1997) *Mol Pharmacol* 52:613
35. Schreiber SL, Chen J, Hung DT (1996) *Chem Biol* 3:287
36. Martello LA, McDaid HM, Regl DL, Yang CH, Meng D, Pettus TRR, Kaufman MD, Arimoto H, Danishefsky SJ, Smith AB, Horowitz SB (2000) *Clin Cancer Res* 6:1978
37. Huang GS, Lopez-Barcons L, Freeze BS, Smith AB, Goldberg GL, Horwitz SB, McDaid HM (2006) *Clin Cancer Res* 12:298
38. Sanchez-Pedregal VM, Kubicek K, Meiler J, Lyothier I, Paterson I, Carlomagno T (2006) *Angew Chem Intl Ed* 45:7388
39. Mita A, Lockhart C, Chen TL, Bocinski K, Curtright J, Cooper W, Hammond L, Rothenberg M, Rowinsky E, Sharma S (2004) *ASCO Annual Meeting Proceedings (Post-Meeting Edition)* *J Clin Oncol* 22(14S) (July 15 Suppl) Abstract 2025
40. Altaha R, Fojo T, Reed E, Abraham J (2002) *Curr Pharm Design* 8:1707
41. <http://www.fda.gov/bbs/topics/NEWS/2007/NEW01732.html>
42. Piel J (2004) *Nat Prod Rep* 21:519
43. Nerenberg JB, Hung DT, Somers PK, Schreiber SL (1993) *J Am Chem Soc* 115:12621

44. Hung DT, Nerenberg JB, Schreiber SL (1996) *J Am Chem Soc* 118:11054
45. Smith AB, Qiu YP, Jones DR, Kobayashi K (1995) *J Am Chem Soc* 117:12011
46. Smith AB, Beauchamp TJ, LaMarche MJ, Kaufman MD, Qiu YP, Arimoto H, Jones DR, Kobayashi K (2000) *J Am Chem Soc* 122:8654
47. Smith AB, Kaufman MD, Beauchamp TJ, LaMarche MJ, Arimoto H (1999) *Org Lett* 1:1823
48. Smith AB, Kaufman MD, Beauchamp TJ, LaMarche MJ, Arimoto H (2000) *Org Lett* 2:1983
49. Smith AB, Freeze BS, Brouard I, Hirose T (2003) *Org Lett* 5:4405
50. Smith AB, Freeze BS, Xian M, Hirose T (2005) *Org Lett* 7:1825
51. Harried SS, Yang G, Strawn MA, Myles DC (1997) *J Org Chem* 62:6098
52. Harried SS, Lee CP, Yang G, Lee TIH, Myles DC (2003) *J Org Chem* 68:6646
53. Marshall JA, Johns BA (1998) *J Org Chem* 63:7885
54. Marshall JA, Lu ZH, Johns BA (1998) *J Org Chem* 63:817
55. Paterson I, Florence GJ, Gerlach K, Scott JP (2000) *Angew Chem Intl Ed* 39:377
56. Paterson I, Florence GJ (2000) *Tetrahedron Lett* 41:6935
57. Paterson I, Florence GJ, Gerlach K, Scott JP, Sereinig N (2001) *J Am Chem Soc* 123:9535
58. Paterson I, Delgado O, Florence GJ, Lyothier I, Scott JP, Sereinig N (2003) *Org Lett* 5:35
59. Paterson I, Delgado O, Florence GJ, Lyothier I, O'Brien M, Scott JP, Sereinig N (2005) *J Org Chem* 70:150
60. Paterson I, Lyothier I (2004) *Org Lett* 6:4933
61. Paterson I, Lyothier I (2005) *J Org Chem* 70:5494
62. Arefolov A, Panek JS (2005) *J Am Chem Soc* 127:5596
63. Arefolov A, Panek JS (2002) *Org Lett* 4:2397
64. de Lemos E, Porée FH, Commerçon A, Betzer JF, Pancrazi A, Ardisson J (2007) *Angew Chem Intl Ed* 46:1917
65. Mickel SJ, Sedelmeier GH, Niederer D, Daeffler R, Osmani A, Schreiner K, Seeger-Weibel M, Bérød B, Schaer K, Gamboni R, Chen S, Chen W, Jagoe CT, Kinder FR, Loo M, Prasad K, Repic O, Shieh W-C, Wang R-M, Waykole L, Xu DD, Xue S (2004) *Org Process Res Dev* 8:92
66. Mickel SJ, Sedelmeier GH, Niederer D, Schuerch F, Grimler D, Koch G, Daeffler R, Osmani A, Hirni A, Schaer K, Gamboni R, Bach A, Chaudhary A, Chen S, Chen W, Hu B, Jagoe CT, Kim H-Y, Kinder FR, Liu Y, Lu Y, McKenna J, Prasad M, Ramsey T M, Repic O, Rogers L, Shieh W-C, Wang R-M, Waykole L (2004) *Org Process Res Dev* 8:101
67. Mickel SJ, Sedelmeier GH, Niederer D, Schuerch F, Koch G, Kuesters E, Daeffler R, Osmani A, Seeger-Weibel M, Schmid E, Hirni A, Schaer K, Gamboni R, Bach A, Chen S, Chen W, Geng P, Jagoe CT, Kinder FR, Lee GT, McKenna J, Ramsey TM, Repic O, Rogers L, Shieh W-C, Wang R-M, Waykole L (2004) *Org Process Res Dev* 8:107
68. Mickel SJ, Sedelmeier GH, Niederer D, Schuerch F, Seger M, Schreiner K, Daeffler R, Osmani A, Bixel D, Loiseleur O, Cercus J, Stettler H, Schaer K, Gamboni R, Bach A, Chen G-P, Chen W, Geng P, Lee GT, Loeser E, McKenna J, Kinder FR, Königsberger K, Prasad K, Ramsey TM, Reel N, Repic O, Rogers L, Shieh W-C, Wang R-M, Waykole L, Xue S, Florence G, Paterson I (2004) *Org Process Res Dev* 8:113
69. Mickel SJ, Niederer D, Daeffler R, Osmani A, Kuesters E, Schmid E, Schaer K, Gamboni R, Chen W, Loeser E, Kinder FR, Königsberger K, Prasad K, Ramsey TM, Repic O, Wang R-M, Florence G, Lyothier I, Paterson I (2004) *Org Process Res Dev* 8:122
70. Paterson I, Wren SP (1993) *J Chem Soc Chem Commun* 1790
71. Clark DL, Heathcock CH (1993) *J Org Chem* 58:5878
72. Golec JMC, Jones SD (1993) *Tetrahedron Lett* 34:8159
73. Evans PL, Golec JMC, Gillespie RJ (1993) *Tetrahedron Lett* 34:8163
74. Golec JMC, Gillespie RJ (1993) *Tetrahedron Lett* 34:8167
75. Paterson I, Schlapbach A (1995) *Synlett* 498
76. Miyazawa M, Oonuma S, Maruyama K, Miyashita M (1997) *Chem Lett* 1191
77. Miyazawa M, Oonuma S, Maruyama K, Miyashita M (1997) *Chem Lett* 1193
78. Misske AM, Hoffmann HMR (1999) *Tetrahedron* 55:4315
79. Evans DA, Halstead DP, Allison BD (1999) *Tetrahedron Lett* 40:4461

80. Filla SA, Song JJ, Chen LR, Masamune S (1999) *Tetrahedron Lett* 40:5449
81. Yadav JS, Abraham S, Reddy MM, Sabitha G, Sankar AR, Kunwar AC (2001) *Tetrahedron Lett* 42:4713. Correction (2002) *Tetrahedron Lett* 43:3453
82. Arjona O, Menchaca R, Plumet J (2001) *Tetrahedron* 57:6751
83. BouzBouz S, Cossy J (2001) *Org Lett* 3:3995
84. Chakraborty TK, Laxman P (2001) *J Indian Chem Soc* 78:543
85. Shahid KA, Li YN, Okazaki M, Shuto Y, Goto F, Kiyooka S (2002) *Tetrahedron Lett* 43:6373
86. Shahid KA, Mursheda J, Okazaki M, Shuto Y, Goto F, Kiyooka S (2002) *Tetrahedron Lett* 43:6377. Correction (2003) *Tetrahedron Lett* 44:1519
87. Day BW, Kangani CO, Avor KS (2002) *Tetrahedron-Asymmetry* 13:1161
88. Yakura T, Kitano T, Ikeda M, Uenishi J (2003) *Heterocycles* 59:347
89. Kiyooka S-I, Shahid KA, Goto F, Okazaki M, Shuto Y (2003) *J Org Chem* 68:7967
90. Francavilla C, Chen W, Kinder FR (2003) *Org Lett* 5:1233
91. Baz àn-Tejeda B, Georgy M, Campagne J-M (2004) *Synlett* 720
92. Loiseleur O, Koch G, Wagner T (2004) *Org Process Res Dev* 8:597
93. BouzBouz S, Cossy J (2004) *Synlett* 2034
94. Ramachandran PV, Prabhudas B, Chandra JS, Reddy MVR (2004) *J Org Chem* 69:6294
95. Loiseleur O, Koch G, Cercus J, Schürch F (2005) *Org Process Res Dev* 9:259
96. Parker KA, Cao H (2006) *Org Lett* 8:3541
97. Burlingame MA, Mendoza E, Ashley GW, Myles DC (2006) *Tetrahedron Lett* 47:1209
98. Aicher TD, Kishi Y (1987) *Tetrahedron Lett* 28:3463
99. Takai K, Kuroda T, Nakatsukasa S, Oshima K, Nozaki H (1985) *Tetrahedron Lett* 26:5585
100. Takai K, Tagashira M, Kuroda T, Oshima K, Utimoto K, Nozaki H (1986) *J Am Chem Soc* 108:6048
101. Jin H, Uenishi J, Christ WJ, Kishi Y (1986) *J Am Chem Soc* 108:5644
102. Roush WR, Palkowitz AD, Ando K (1990) *J Am Chem Soc* 112:6348
103. Evans DA, Gauchet-Prunet JA (1993) *J Org Chem* 58:2446
104. Stork G, Zhao K (1989) *Tetrahedron Lett* 30:2173
105. Negishi E, Valente LF, Kobayashi M (1980) *J Am Chem Soc* 102:3298
106. Still WC, Gennari C (1983) *Tetrahedron Lett* 24:4405
107. Hung DT, Nerenberg JB, Schreiber SL (1994) *Chem Biol* 1:67
108. Evans DA, Bartoli JA, Shih TL (1981) *J Am Chem Soc* 103:2127
109. Evans DA, Takacs JM, McGee LR, Ennis MD, Mathre DJ, Bartoli JA (1981) *Pure Appl Chem* 53:1109
110. Gage JR, Evans DA (1990) *Org Syn* 68:77
111. Gage JR, Evans DA (1990) *Org Syn* 68:83
112. Chen J, Wang T, Zhao K (1994) *Tetrahedron Lett* 35:2827
113. Arimoto H, Kaufman MD, Kobayashi K, Qiu YP, Smith AB (1998) *Synlett* 765
114. Evans DA, Chapman KT, Carreira EM (1998) *J Am Chem Soc* 110:3560
115. Ikeda Y, Ukai J, Ikeda N, Yamamoto H (1987) *Tetrahedron* 43:723
116. Miyaura N, Suzuki A (1995) *Chem Rev* 95:2457
117. Brown HC, Bhat KS (1986) *J Am Chem Soc* 108:293
118. Danishefsky SJ, Larson E, Askin D, Kato N (1985) *J Am Chem Soc* 107:1246
119. Luche JL, Gemal AL (1979) *J Am Chem Soc* 101:5848
120. Gemal AL, Luche JL (1981) *J Am Chem Soc* 103:5454
121. Ferrier RJ (1964) *J Chem Soc* 5443
122. Keck GE, Abbott DE (1984) *Tetrahedron Lett* 25:1883
123. Linderman RJ, Cusack KP, Jaber MR (1996) *Tetrahedron Lett* 37:6649
124. White JD, Nylund CS, Green NJ (1997) *Tetrahedron Lett* 38:7329
125. Roush WR, Grover PT (1992) *Tetrahedron* 48:1981
126. Tsai DJ-S, Matteson DS (1981) *Tetrahedron Lett* 22:2751
127. Chen CP, Tagami K, Kishi Y (1995) *J Org Chem* 60:5386

128. Marshall JA, Perkins JF, Wolf MA (1995) *J Org Chem* 60:5556
129. Marshall JA, Palovich MR (1997) *J Org Chem* 62:6001
130. Paterson I, Norcross RD, Ward RA, Romea P, Lister MA (1994) *J Am Chem Soc* 116:11287
131. Paterson I, Wallace DJ, Cowden CJ (1998) *Synthesis* 639
132. Paterson I, Lister MA (1988) *Tetrahedron Lett* 29:585
133. Paterson I, Channon J (1992) *Tetrahedron Lett* 33:797
134. Paterson I, Tillyer RD (1992) *Tetrahedron Lett* 33:4233
135. Paterson I, Goodman JM, Isaka M (1989) *Tetrahedron Lett* 30:7121
136. Paterson I, Arnott EA (1998) *Tetrahedron Lett* 39:7185
137. Paterson I, Wallace DJ, Velázquez SM (1994) *Tetrahedron Lett* 35:9083
138. Paterson I, Wallace DJ (1994) *Tetrahedron Lett* 35:9087
139. Cowden CJ, Paterson I (1997) *Org React* 51:1
140. Carling RW, Holmes AB (1986) *J Chem Soc Chem Commun* 325
141. Curtis NR, Holmes AB, Looney MG (1991) *Tetrahedron* 47:7171
142. Holmes AB, Looney MG (1993) *J Am Chem Soc* 115:5815
143. Fuhry MAM, Holmes AB, Marshall DR (1993) *J Chem Soc Perkin Trans* 1:2743
144. Burton JW, Clark JS, Derrer S, Stork TC, Bendall JG, Holmes AB (1999) *Synlett* 972
145. Paterson I, Perkins MV (1996) *Tetrahedron* 52:1811
146. Paterson I, Perkins MV (1992) *Tetrahedron Lett* 33:801
147. Pirrung MC, Heathcock CH (1980) *J Org Chem* 45:1727
148. Paterson I (1983) *Tetrahedron Lett* 24:1311
149. De Mico A, Margarita R, Parlanti L, Vescovi A, Piancatelli G (1997) *J Org Chem* 62:6974
150. Paterson I, Goodman JM, Lister MA, Schumann RC, McClure CK, Norcross RD (1990) *Tetrahedron* 46:4663
151. Paterson I, Cumming JG, Smith JD, Ward RA (1994) *Tetrahedron Lett* 35:441
152. Paterson I, Oballa RM, Norcross RD (1996) *Tetrahedron Lett* 37:8581
153. Paton, RS, Goodman JM (2006) *Org Lett* 8:4299
154. Wensheng Y, Su M, Jin Z (1999) *Tetrahedron Lett* 40:6725
155. Jain NF, Takenaka N, Panek JS (1996) *J Am Chem Soc* 118:12475
156. Jain NF, Crillo PF, Pelletier R, Panek JS (1995) *Tetrahedron Lett* 36:8727
157. Masse CE, Panek JS (1995) *Chem Rev* 95:1293
158. Panek JS, Beresis RT (1993) *J Org Chem* 58:809
159. Panek JS, Crillo PF (1993) *J Org Chem* 58:294
160. Hart DW, Schwartz J (1974) *J Am Chem Soc* 96:8115
161. Buchwald SL, LaMaire SJ, Nielsen RB, Watson BT, King SM (1987) *Tetrahedron Lett* 28:3895
162. Paterson I, Gibson KR, Oballa, RM (1996) *Tetrahedron Lett* 47:8585
163. Evans DA, Coleman PJ, Côté B (1997) *J Org Chem* 62:788
164. Evans DA, Hoveyda AH (1990) *J Am Chem Soc* 112:6447
165. Tomioka H, Takai K, Oshima K, Nozaki H (1981) *Tetrahedron Lett* 22:1605
166. Hoppe D (1984) *Angew Chem* 96:930
167. Hoppe D, Hense T (1997) *Angew Chem* 109:2376
168. Hoppe D, Zchage O (1989) *Angew Chem* 101:67
169. Hoppe D, Zchage O (1992) *Tetrahedron* 48:8389
170. Fargeas V, Le Ménez P, Berque I, Ardisson J, Pancrazi A (1996) *Tetrahedron* 52:6613
171. Berque I, Le Ménez P, Razon P, Mahuteau J, Férézou J-P, Pancrazi A, Ardisson J, Brion J-D (1999) *J Org Chem* 64:373
172. Kocienski P, Wadman S, Cooper K (1989) *J Am Chem Soc* 111:2363
173. Kocienski P, Barber C (1990) *Pure Appl Chem* 62:1933
174. Le Ménez P, Fargeas V, Berque I, Poisson J, Ardisson J, Lallem JY, Pancrazi A (1995) *J Org Chem* 60:3592
175. Fargeas V, Le Ménez P, Berque I, Ardisson J, Pancrazi A (1996) *Tetrahedron* 52:6613
176. Braun M (1998) *Angew Chem Int Ed* 37:430

- 177. Knorr R (2004) *Chem Rev* 104:3795
- 178. Corey EJ, Bakshi RK, Shibata S (1987) *J Am Chem Soc* 109:5551
- 179. Kaminski ZJ (1987) *Synthesis* 10:917
- 180. Kaminski ZJ, Paneth P, Rudzinski J (1998) *J Org Chem* 63:424
- 181. Mickel SJ, Daeffler R, Prikoszovich W (2005) *Org Process Res Dev* 9:113
- 182. Panek JS, Beresis RT, Xu F, Yang M (1991) *J Org Chem* 56:7391

Tubulin-Binding Agents

Synthetic, Structural and Mechanistic Insights

Carlomagno, T. (Ed.)

2009, XI, 331 p., Hardcover

ISBN: 978-3-540-69036-8